58. ... I. Chernobyl'ska... and I. M. Tadaiko, Heat exchange during boiling of liquids in narrow annular tubes. *Sov. Phys.—Tech. Phys. (Engl. Transl.)* **1**, 1244 (1956).
59. K. Nishikawa, H. Kusuda, K. Yamasaki, and K. Tanaka, Nucleate boiling at low liquid levels. *Bull. JSME* **10**, 328 (1967).
60. H. Kusuda and K. Nishikawa, A study on nucleate boiling in liquid film. *Mem. Fac. Eng. Kyushu Univ.* **27**, 155 (1967).
61. K. Nishikawa and T. Ito, Augmentation of nucleate boiling heat transfer by prepared surfaces. *In* "Heat Transfer in Energy Problems," p. 119. Hemisphere, Washington, D.C., 1983.
62. K. Nishikawa, T. Ito, and K. Tanaka, Augmented heat transfer by nucleate boiling at prepared surfaces. *Proc. ASME–JSME Therm. Eng. Conf.* **1**, 386 (1983).
63. K. Nishikawa and T. Ito, Augmentation performance of boiling heat transfer. *In* "Research on Effective Use of Thermal Energy," Vol. 1, SPEY 1, p. 39. Minist. Educ. Sci. Cult., Tokyo.
64. Sales catalogue of Hitachi Cable, Cat. No. EA 501 (1987).
65. N. Arai, T. Fukushima, A. Arai, T. Nakajima, K. Fujie, and Y. Nakayama, Heat transfer tubes enhancing boiling and condensation in heat exchangers of a refrigerating machine. *ASHRAE Trans.* **83**, 58 (1977).
66. W. Nakayama, T. Daikoku, H. Kuwahara, and T. Nakajima, Dynamic model of enhanced boiling heat transfer on porous surface. *J. Heat Transfer* **102**, 445 (1980).
67. A. M. Czikk, C. F. Gottzmann, E. G. Ragi, J. G. Withers, and E. P. Habdas, Performance of advanced heat transfer tubes in refrigerant-flooded liquid coolers. *ASHRAE Trans.* **76**, 96 (1970).
68. C. F. Gottzmann, P. S. O'Neil, and P. F. Minton, High efficiency heat exchangers. *Chem. Eng. Prog.* **69**, 69 (1973).
69. P. S. O'Neil, C. F. Gottzmann, and J. W. Terbot, Heat exchanger for NGL. *Chem. Eng. Prog.* **67**, 80 (1971).
70. K. Nishikawa, T. Ito, S. Yoshida, and Y. Fujita, Development of the highest performance boiling surface and its application to heat exchanger. *In* "Research on Effective Use of Thermal Energy," SPEY 14, p. 21. Minist. Educ., Sci. Cult. Tokyo.

Two-Phase Slug Flow

YEHUDA TAITEL AND DVORA BARNEA

Faculty of Engineering, Department of Fluid Mechanics and Heat Transfer, Tel-Aviv University, Ramat-Aviv 69978, Israel

I. Introduction

Gas–liquid flow in conduits may take on a variety of configurations related to the spatial distribution of the two phases in the pipe, termed as flow patterns (Mandhane *et al.*, 1974; Taitel and Dukler, 1976; Taitel *et al.*, 1980; Barnea, 1987; Weisman *et al.*, 1979). One of the most complex flow pattern with unsteady characteristics is the intermittent or slug flow. Gas–liquid intermittent flow exists in the whole range of pipe inclination and over a wide range of gas and liquid flow rates. In vertical slug flow most of the gas is located in large bullet-shaped bubbles, which occupy most of the pipe cross section. These bubbles are usually called Taylor bubbles. The Taylor bubbles are separated by liquid slugs containing usually small bubbles. The liquid confined between the bubble and the pipe wall flows around the Taylor bubble in a thin falling film. In horizontal and inclined flow, slugs of liquid that fill the whole cross section of the pipe are separated by a stratified zone with an elongated gas bubble in the upper part of the pipe and the liquid film at the bottom. The intermittent pattern is sometimes subdivided into slug and elongated bubble flow patterns. When the flow is calm and the liquid slug is almost free of gas bubbles the pattern is termed as elongated bubble flow. For high flow rates, when the liquid is aerated with gas bubbles, the flow is designated as slug flow. In spite of the distinction between slug and elongated bubble flows, the term *slug flow* is still often used for the general intermittent flow.

Slug flow is a highly complex type of flow with an unsteady nature, thus the prediction of pressure drop, heat, and mass transfer for such flow is a difficult task. Obviously an exact solution of the continuum equations is out of the question at this time. Therefore a variety of approximate methods

Copyright © 1990 by Academic Press, Inc.
All rights of reproduction in any form reserved.

has been developed for calculating the slug hydrodynamic parameters. The former methods simply used correlations of experimental results. More recently there is a tendency to formulate approximate models that are capable of simulating the flow behavior sufficiently accurate so that the calculation of the pressure drop as well as other flow parameters can be performed with a relatively high degree of confidence and generality. Such models were introduced by Dukler and Hubbard (1975) and Nicholson *et al.* (1978) for horizontal flow; Fernandes *et al.* (1983), Sylvester (1987), and Orell and Rembrand (1986) for vertical flow; and Bonnecaze *et al.* (1971) for the inclined flow.

All of the aforementioned models deal with steady slug flow, which is an orderly flow with relatively short slugs (less than $100D$) and a constant average flow rate of liquid and gas over the time period of a slug cycle.

There are, however, more complex types of slugs that are of a typical transient nature and are abnormally long. The most common are the terrain-induced slugging, where slugs are generated in a pipeline when the heavy liquid is accumulated in the lower section of a pipe that follows a hilly terrain. The state of the art of transient slugging is not yet well developed and perhaps only the simple case of a system that contains a single riser and a single pipeline was adequately studied (Schmidt *et al.*, 1980; Taitel, 1986; Taitel *et al.*, 1989).

In this Chapter we will treat first the steady slug flow. Various options of modeling the hydrodynamic parameters and pressure drop will be introduced using a unified approach that is applicable for the vertical, horizontal, as well as the inclined cases. Transient phenomena in slug flow will also be reviewed with the detailed example of the case of severe slugging in a pipeline–riser system. This system is of major practical importance for the offshore oil and gas industry. It is also the one that has been treated with sufficient success.

Heat transfer in slug flow is also of major importance for practical applications. The topic of heat transfer during evaporation and condensation is considered in the specialized literature. The treatment of the two-phase flow is usually considered there as a two-phase mixture. Very few studies have been performed that treat the liquid and the gas in slug flow as different entities and that address themselves to questions such as the temperature profiles in the liquid and the gas, the local fluctuation of the wall temperature, the difference between the upper and lower parts of the wall temperature in slug flow, and the heat-transfer coefficient in slug flow with dependence on peripherial and axial positions. Since we feel that the amount of work done on this subject is not yet at the point where a meaningful, coherent summary can be written, this review is limited to the hydrodynamic aspects of slug flow only. Note, however, that the hydrodynamics of slug flow is the basis for any detailed heat-transfer analysis.

II. Steady-State Slug-Flow Modeling

Models for predicting the steady slug flow were usually treated separately for the horizontal case and for the vertical case. Some papers also consider the inclined case.

For the horizontal case, the most detailed models were presented by Dukler and Hubbard (1975) and Nicholson *et al.* (1978). For vertical upwards flow, the most detailed work has been done by Fernandes *et al.* (1983), Sylvester (1987), and Orell and Rembrand (1986). The inclined case was considered by Bonnecaze *et al.* (1971).

In this presentation, we are not going to describe previous work in any consecutive manner. We will rather present our own approach to the modeling of slug flow that we feel is the best combination of engineering accuracy and ease of calculation. Previous work will be reviewed (in a critical way when appropriate) as we move along in the development of modeling the different mechanisms that take place in slug flow. We will try to present an approach that is as general as possible and can handle vertical, horizontal, and inclined slug flows in an unified fashion.

Slug flow is a very complex fluid-mechanics problem. The purpose of modeling slug flow is to be fairly close to the true physical process that is taking place, but it is also important for a model to be simple enough so that practical solutions for the slug-flow parameters can be obtained with reasonable effort and that the modeling could be used in routine engineering calculations.

The schematic geometry of slug flow is shown in Figure 1. The slug body is subdivided into two main sections: the liquid slug zone of length l_s and the film zone of length l_f. Although the liquid slug zone can be aerated by dispersed bubbles, it forms a competent bridging and gas cannot penetrate through the slug zone. The liquid holdup within the liquid slug zone is designated as R_s. Once the slug is incapable of forming a competent bridging, the slugs are then termed protoslugs (Andritsos and Hanratty, 1987) or wavy annular (Barnea *et al.*, 1980), and this is the beginning of transition to annular flow. The average liquid velocity in the liquid slug body is designated as u_L. The average axial velocity of the dispersed bubbles in the liquid slug is termed u_b. Note that u_L and u_b are not necessarily the same, even though for horizontal flow, both velocities are considered equal.

The film zone consists of a liquid film and an elongated gas bubble. For horizontal and inclined pipes, the bubble is in the upper part of the pipe. In vertical and off-vertical pipes, a complete symmetry is assumed, the bubble is in the center of the pipe and a thin film flows around it adjacent to the pipe wall. In this case the large bubble is termed Taylor bubble, and the film zone is usually termed the Taylor bubble zone. The translational

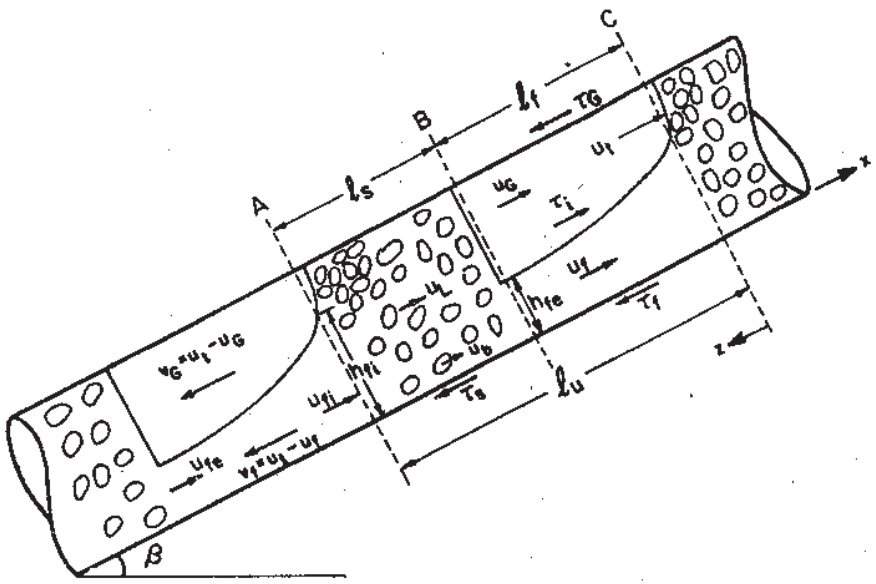

FIG. 1. Slug-flow geometry.

velocity of the elongated bubble u_t is the velocity at which the elongated bubble propagates downstream. If one moves at a velocity u_t the slug picture is seen as frozen in space. The liquid velocity in the film is designated as u_f and that of the gas u_G. Note that unlike the liquid slug region, which is considered axially homogeneous, the liquid and gas velocities in the film zone vary along the pipe due to the variation of the film thickness, $h_f(z)$ or $\delta(z)$ (for the symmetrical–vertical case), behind the liquid slug.

A. Mass Balances

Mass balances presented here consider both the liquid and gas as incompressible. For long pipelines, where the density is not constant, we can still consider it as locally constant for the purpose of calculating steady slug flow.

A liquid mass balance over a slug unit can be performed in two ways. One way is to integrate the fluid flow rate at a fixed cross section over the time of the passage of a slug unit. The second one is by considering the volume of fluid in a slug unit. Both methods obviously yield the same results.

Using the first approach for the liquid mass balance yields

$$W_L = \frac{1}{t_u}\left(u_L A R_s \rho_L t_s + \int_0^{t_u} u_f A R_f \rho_L \, dt\right) \tag{1}$$

where W_L is the input liquid flow rate; u_L is the liquid average velocity in the liquid slug; u_f is the liquid velocity in the film; t_u, t_s, and t_f are the times for the passage of the slug unit, the liquid slug, and the film zone, respectively. Since $t_s = l_s/u_t$ and $t_f = l_f/u_t$, Eq. (1) takes the form

$$W_L = u_L A R_s \rho_L \frac{l_s}{l_u} + \frac{1}{l_u}\int_0^{l_f} u_f A R_f \rho_L \, dx \tag{2}$$

The second way of formulating the mass balance yields the following relation,

$$W_L = \frac{1}{t_u}\left(\rho_L A R_s l_s + \int_0^{l_f} \rho_L A R_f \, dx\right) - X \tag{3}$$

The term in the parenthesis is the mass of the liquid in a slug unit. A slug unit is propagating in the pipe at a velocity u_t and the time for a slug unit to pass through a fixed point in the pipe is $t_u = l_u/u_t$. However, at this time, part of the liquid in the film moves upstream (backward) relative to the gas–liquid interface and is captured by the following slug. This amount of picked up liquid X is given by the expression

$$X = (u_t - u_L)\rho_L A R_s = (u_t - u_f)\rho_L A R_f \tag{4}$$

Using Eq. (4) for X, one can show that both Eqs. (1) and (2) are indeed the same.

Equations (2) and (4) can be combined to yield

$$u_{LS} = u_L R_s + u_t(1 - R_s)\frac{l_f}{l_u} - \frac{u_t}{l_u}\int_0^{l_f} \alpha_f \, dx \tag{5}$$

Exactly equivalent mass balances can be performed on the gas. However, it is more convenient to use a mass balance on one species only and a mass balance on the mixture. A very simple continuity balance on both liquid and gas states that for contant densities, the volumetric flow rate through any cross section is constant. Applying this balance on a cross section in the liquid slug zone yields

$$u_s = u_{LS} + u_{GS} = u_L R_s + u_b \alpha_s \tag{6}$$

where u_s is the mixture velocity within the liquid slug.

B. Average Void Fraction

The average void fraction of a slug unit is defined as

$$\alpha_u = (\alpha_s l_s + \int_0^{l_f} \alpha_f dx)/l_u \tag{7}$$

Using the mass balance [Eq. (5)] to eliminate the integral term in Eq. (7) yields

$$\alpha_u = (-u_{LS} + u_L R_s + u_t \alpha_s)/u_t \tag{8}$$

Using Eq. (6), the liquid flow rate u_{LS} can be replaced by u_{GS} to yield

$$\alpha_u = (u_{GS} - u_b \alpha_s + u_t \alpha_s)/u_t \tag{9}$$

As pointed out before (Barnea, 1989), Eqs. (8) and (9) present indeed a very interesting result. It shows that the average void fraction of a slug unit depends only on the liquid and gas flow rates (u_{GS}, u_{LS}), the dispersed bubble velocity u_b, the translational velocity u_t, and the void fraction within the liquid slug α_s, and it is independent of the bubble shape, the bubble length, the liquid slug length, and film thickness. This is a very important and convenient result since it shows that the gravitational pressure drop can be calculated independent of the detailed slug structure. For the simple case when the liquid slug is not aerated, $R_s = 1$ and Eq. (9) reduces to the simple result $\alpha_u = u_{GS}/u_t$.

C. Hydrodynamics of the Liquid Film

The length of the liquid film l_f, its shape $h_f(z)$, the velocity profile along the liquid film $u_f(z)$, and, especially, the film thickness and its velocity just before pickup h_{fe} and u_{fe}, respectively, are important parameters for calculating the pressure drop and heat and mass transfer in slug flow.

The shape of the liquid film is a very complex structure, especially near the tail of the liquid slug. It is a three-dimensional problem, with free surface, of turbulent flow and obviously an exact solution is out of the question at this time. A reasonable approximation is to use the one-dimensional approach of the channel flow theory. This method has been used by Dukler and Hubbard (1975) and Nicholson *et al.* (1978).

In order to find solutions for the film velocity u_f and the film holdup R_f as a function of position from the rear of the slug, z, we will consider momentum balances on the film zone. Refering to Figure 1, the momentum equations for the liquid film and the gas above it relative to a coordinate system moving with a velocity u_t are

$$\rho_L \nu_f \frac{\partial \nu_f}{\partial z} = -\frac{\partial P}{\partial z} + \frac{\tau_f S_f}{A_f} - \frac{\tau_i S_i}{A_f} + \rho_L g \sin\beta - \rho_L g \cos\beta \frac{\partial h_f}{\partial z} \tag{10}$$

$$\rho_G \nu_G \frac{\partial \nu_G}{\partial z} = -\frac{\partial P}{\partial z} + \frac{\tau_G S_G}{A_G} + \frac{\tau_i S_i}{A_G} + \rho_G g \sin\beta - \rho_G g \cos\beta \frac{\partial h_f}{\partial z} \tag{11}$$

where $\nu_f = u_t - u_f$ and $\nu_G = u_t - u_G$. Note that although these equations are written for the relative velocities ν_f and ν_G, the shear stresses are given in terms of the real velocities as follows (see Fig. 1 for the definition of the positive direction for the shear stresses):

$$\tau_f = f_f(\rho_L |u_f| u_f/2) \tag{12}$$

$$\tau_G = f_G(\rho_G |u_G| u_G/2) \tag{13}$$

$$\tau_i = f_i[\rho_G |u_G - u_f| (u_G - u_f)/2] \tag{14}$$

where f_f, f_G, and f_i are the friction factors between the liquid and the wall, the gas and the wall, and the gas–liquid interface, respectively; u_f and u_G are considered positive in the downstream (x) direction.

For smooth pipes, the Blasius correlation can be used,

$$f_f = C_f(D_h u_f/\nu_L)^n \tag{15}$$

where $D_h = 4A_f/S_f$. A similar expression can be used for the gas with the exception that the gas hydraulic diameter is taken as $D_h = 4A_G/(S_G + S_i)$ (Taitel and Dukler, 1976). For laminar flow $C_f = 16$ and $n = -1$, while for turbulent flow $C_f = 0.046$ and $n = -0.2$.

For rough pipes the roughness of the pipe should be taken into account. An example for such an expression is the convenient explicit formula (Hall, 1957):

$$f = 0.001375\{1 + [2 \times 10^4(\varepsilon/D_h) + (10^6/\mathrm{Re})]^{1/3}\} \tag{16}$$

Obviously many other correlations can be used.

More problematic is the determination of the interfacial friction factor f_i. For the case of low liquid and gas velocities, the smooth surface friction factor can be used. When the interface is wavy, the wavy structure determines the value of the average friction factor. Unfortunately, due to the complexity of the wavy structure, the interfacial friction factor cannot be predicted accurately and one has to use some crude correlations and assumptions. The nature of the interface (smooth or wavy) can be determined on the basis of flow pattern maps considering the film zone as stratified flow with the appropriate flow rates of liquid and gas.

For wavy stratified flow in the horizontal and inclined cases, a constant value of $f_i = 0.014$ was suggested (Cohen and Hanratty, 1968; Shoham and Taitel, 1984). For the vertical case Wallis (1969) correlation for cocurrent annular flow

$$f_i = 0.005[1 + 300(\delta/D)] \tag{17}$$

can be used, though the flow in the film zone is usually countercurrent. It may be noted that Wallis *et al.* (1978, 1979) suggested modified correlations for countercurrent flow. However, those correlations are applicable near the flooding point and this is usually not the case for normal slug flow.

As can be seen, the information regarding the interfacial shear is very limited, primarily for inclined pipes. Fortunately the accuracy of the interfacial friction is generally not important since in most cases the interfacial shear in the film zone is negligible.

Eliminating the pressure gradient from Eq. (10) and (11) yields

$$\rho_L \nu_f \frac{\partial \nu_f}{\partial z} - \rho_G \nu_G \frac{\partial \nu_G}{\partial z} = \frac{\tau_f S_f}{A_f} - \frac{\tau_G S_G}{A_G} - \tau_i S_i \left(\frac{1}{A_f} + \frac{1}{A_G}\right) + (\rho_L - \rho_G) g \sin\beta - (\rho_L - \rho_G) g \cos\beta \frac{\partial h_f}{\partial z} \tag{18}$$

Using Eq. (4), the relative velocities ν_f and ν_G are given by

$$\nu_f \equiv (u_t - u_f) = (u_t - u_L) R_s / R_f \tag{19}$$

Likewise

$$\nu_G \equiv (u_t - u_G) = (u_t - u_b) \alpha_s / \alpha_f \tag{20}$$

Since R_f as well as α_f are functions of h_f or δ, substituting these values in Eq. (18) yields a differential equation for h_f (or δ) as a function of z:

$$\frac{dh_f}{dz} = \frac{\dfrac{\tau_f S_f}{A_f} - \dfrac{\tau_G S_G}{A_G} - \tau_i S_i \left(\dfrac{1}{A_f} + \dfrac{1}{A_G}\right) + (\rho_L - \rho_G) g \sin\beta}{(\rho_L - \rho_G) g \cos\beta - \rho_L \nu_f \dfrac{(u_t - u_L) R_s}{R_f^2} \dfrac{dR_f}{dh_f} - \rho_G \nu_G \dfrac{(u_t - u_b)(1 - R_s)}{(1 - R_f)^2} \dfrac{dR_f}{dh_f}} \tag{21}$$

where for the case of stratified film flow

$$\frac{dR_f}{dh_f} = \frac{4}{\pi D} \sqrt{1 - \left(2\frac{h_f}{D} - 1\right)^2} \tag{22}$$

The differential equation [Eq. (21)] is solved numerically for $h_f(z)$ and the corresponding $u_f(z)$ is found using the mass balance [Eq. (19)]. The integration is performed until the mass balance of Eq. (5) is satisfied, yielding the length of the liquid film l_f, as well as the holdup R_{fe}, and the velocity u_{fe} at the end of the liquid film just before pickup.

For large z, the limiting value of h_{fe} is the equilibrium liquid level h_E, which is obtained when $dh_f/dz = 0$, namely, the numerator of Eq. (21) equals zero.

Note that for aerated liquid slugs, the gas velocity in the elongated bubbles usually exceeds that of the dispersed bubbles in the liquid bridge. In addition the liquid film seems to be essentially free of small bubbles. The physical picture that is consistent with this description is that the dispersed bubbles in the liquid slug coalesce at the nose of the elongated bubble, while gas bubbles are reentrained from the back of the bubble into the liquid slug. Thus the liquid holdup in the front of the liquid film R_{fi} equals the value of R_s and u_{fi} equal u_L; h_s is the liquid level corresponding to R_s. Thus the integration of Eq. (21) starts normally with $h_f = h_{fi} = h_s$ at $z = 0$ and h_f decreases ($dh_f/dz < 0$) from h_s towards the limit of h_E.

However, under certain conditions, dh_f/dz may be positive. It occurs whenever the critical liquid level h_c is less than h_s, where h_c is the level that equates the denominator to zero. In this case, the liquid level reduces "instantaneously" to the critical level, and the integration of h_f starts with $h_{fi} = h_c$ at $z = 0$. This procedure is similar to the analysis of liquid drainage from a reservoir to a super critical channel flow (Henderson, 1966). We may further note that in the event that h_c or h_s are less than the equilibrium level h_E, then h_E is reached immediately. For the vertical case, the denominator is never zero and a critical film thickness does not exist.

Equation (21) is the most detailed form of the one-dimensional channel flow approach. This approach with several degrees of simplification has been used by various investigators. Dukler and Hubbard (1975) and Nicholson *et al.* (1978) assumed that the pressure drop in the film zone is negligible. Under this assumption, the liquid is treated as an uncoupled free surface channel flow, and Eq. (18) takes the form

$$\rho_L \nu_f (\partial \nu_f / \partial z) = (\tau_f S_f / A_f) + \rho_L g \sin\beta - \rho_L g \cos\beta (\partial h_f / \partial z) \tag{23}$$

Equation (23) is still a differential equation that has to be integrated numerically, and the neglect of the pressure drop along the gas bubble, although usually justified, may be incorrect for very long film zones in which the contribution of the pressure drop in the gas zone is not negligible.

Further simplifications have been proposed in order to avoid the numerical integration. The most common approach is to consider the liquid film

as having a constant thickness in equilibrium. This equilibrium level is indeed the solution of h_E. For the case of the vertical pipe this was, in fact, the only approach taken (Fernandes *et al.*, 1983; Sylvester, 1987; Orell and Rembrand, 1986). In this case, the solution for h (or δ for vertical symmetrical flow) should satisfy

$$\frac{\tau_f S_f}{A_f} - \frac{\tau_G S_G}{A_G} - \tau_i S_i \left(\frac{1}{A_f} + \frac{1}{A_G}\right) + (\rho_L - \rho_G) g \sin\beta = 0 \tag{24}$$

In the aforementioned works, however, the pressure drop in the gas zone was also neglected. This neglect is usually justified only for relatively short bubbles.

In summary, several approaches with various degrees of simplicity have been presented for the hydrodynamics of the liquid film. We focus our attention on three cases:

Case 1. This is the most general formulation for the one-dimensional channel flow approximation. It is given by Eq. (18) or (21).

Case 2. The liquid film is treated as a free surface channel flow [Eq. (23)].

Case 3. An uniform film is assumed along the bubble zone [Eq. (24)].

D. Pressure Drop

Since the slug is not a homogeneous structure, the local axial pressure drop is not constant. For practical purposes, we need the average pressure drop over a slug unit, namely, $\Delta P_u / l_u$.

The pressure drop for a slug unit can be calculated using a global force balance along a slug unit between cuts A–A and B–B (Fig. 1). The momentum fluxes in and out are identical and the pressure drop across this control volume is

$$\Delta P_u = \rho_u g \sin\beta l_u + \frac{\tau_s \pi D}{A} l_s + \int_0^{l_t} \frac{\tau_f S_f + \tau_G S_G}{A} dz \tag{25}$$

where ρ_u is the average density of the slug unit:

$$\rho_u = \alpha_u \rho_G + (1 - \alpha_u)\rho_L \tag{26}$$

The first term on the right-hand side of Eq. (25) is the gravitational contribution to the pressure drop whereas the second and third terms are the frictional term in the slug and in the film zones.

A second method, which is frequently used for calculating the pressure drop, is to neglect the pressure drop in the film region and to calculate the pressure drop only for the liquid slug zone. In the slug zone a control volume between the plane cuts A–A and C–C is used. The resulting pressure drop along a slug unit ΔP_u in this case is

$$\Delta P_u = \rho_s g \sin\beta l_s + \frac{\tau_s \pi D}{A} l_s + \Delta P_{mix} \tag{27}$$

where ρ_s is the average density of the liquid slug body, namely,

$$\rho_s = \alpha_s \rho_G + R_s \rho_L \tag{28}$$

The first term on the right-hand side of Eq. (27) is the gravitational term of the liquid slug; the second term is the pressure loss due to friction, and the third term is the pressure losses in the near-wake region behind the long bubble. Dukler and Hubbard (1975), Nicholson *et al.* (1978), and Stanislav *et al.* (1986) proposed that this pressure drop is associated only with the acceleration of the slow moving liquid in the film to the liquid velocity within the liquid slug, namely,

$$\Delta P_{mix} = \Delta P_{acc} = \rho_L R_s A (u_t - u_L)(u_L - u_{fe}) \tag{29}$$

However, a careful mass balance between cuts A–A and C–C indicates that the contribution to ΔP_{mix} is not only due to the acceleration pressure drop, but also due to the change in the liquid level between the film zone and the liquid slug zone (Taitel and Barnea, 1989), namely,

$$A\,\Delta P_{mix} = \rho_L g \cos\beta \int_0^{h_{fe}} (h_{fe} - y) b\, dy - \rho_L g \cos\beta \int_0^{h_{fi}} (h_{fi} - y) b\, dy + \rho_L R_s A (u_t - u_L)(u_{fi} - u_{fe}) \tag{30}$$

As discussed in the previous section, h_{fi} is usually h_s, and u_{fi} is u_L, in which case the last term on the right-hand side of Eq. (30) is equal to the acceleration pressure drop as given by Eq. (29). However, when $h_c < h_s$, h_{fi} equals h_c, $u_{fi} = u_c$, and the acceleration term in Eq. (30) is different from that in Eq. (29). The integration in Eq. (30) can be carried out and written explicitly

$$\int_0^{h_{fe}} (h_{fe} - y) b\, dy = \frac{D^3}{12} \sqrt{\left[1 - \left(2\frac{h_{fe}}{D} - 1\right)^2\right]^3} + \frac{D^3}{8}\left(2\frac{h_{fe}}{D} - 1\right) \times \left[\frac{\pi}{2} + \sin^{-1}\left(2\frac{h_{fe}}{D} - 1\right) + \left(2\frac{h_{fe}}{D} - 1\right)\sqrt{1 - \left(2\frac{h_{fe}}{D} - 1\right)^2}\right] \tag{31}$$

Inspection of Eq. (30) shows that ΔP_{mix} is always less than ΔP_{acc}. The use of $\Delta P_{mix} = \Delta P_{acc}$ may cause a minor error for small-diameter pipes but it can lead to a serious error when the pipes are of a large diameter.

Two methods have been presented for the pressure-drop calculation. In the first method, a global force balance is used [Eq. (25)], while the second method is based on the momentum balance only on the liquid slug zone, neglecting the pressure drop in the film zone [Eq. (27)]. It will now be shown that the two methods are identical provided that in the first method we also assume that the pressure along the film zone is essentially constant.

The integrated form of the momentum balance given by Eq. (23) is

$$\int_{u_T-u_{fi}}^{u_T-u_{fe}} \rho_L R_f (u_T-u_f)\frac{\partial(u_T-u_f)}{\partial z}\,dz = \int_0^{l_f}\frac{\tau_f S_f}{A}\,dz + \rho_L g\sin\beta \times\int_0^{l_f} R_f\,dz - \rho_L g\cos\beta\int_{h_{fi}}^{h_{fe}} R_f\frac{\partial h_f}{\partial z}\,dz \tag{32}$$

The left-hand side of Eq. (32) is exactly the acceleration term ΔP_{acc}.

Integrating by parts, one can show that

$$\int_0^{h_f} A_f\,dh_f = \int_0^{h_f}(h_f-y)b\,dy \tag{33}$$

Equation (32) then takes the form

$$\rho_L R_s A(u_t-u_L)(u_{fi}-u_{fe}) = \int_0^{l_f}\tau_f S_f\,dz + \rho_L g\sin\beta\int_0^{l_f} A_f\,dz - \rho_L g\cos\beta\int_0^{h_{fe}}(h_{fe}-y)b\,dy + \rho_L g\cos\beta\int_0^{h_{fi}}(h_{fi}-y)b\,dy \tag{34}$$

Substituting Eq. (34) into Eq. (30) yields another expression for ΔP_{mix}:

$$A\,\Delta P_{mix} = \rho_L g\sin\beta\int_0^{l_f} A_f\,dz + \int_0^{l_f}\tau_f S_f\,dz \tag{35}$$

By substituting ΔP_{mix} of Eq. (35) into Eq. (27), one can see that it is identical to Eq. (25) (for the case where pressure drop in the film zone is zero). Namely, the two methods for pressure drop calculation—(1) a global momentum balance on the whole slug unit [Eq. (25)], and (2) a momentum balance over the liquid slug only [Eq. (27)]—are identical.

For upward inclined and vertical flows the equilibrium level (or film thickness) is frequently reached after a short distance from the liquid slug tail. In this case, one can view the liquid film as composed of two sections. A curved zone and an equilibrium zone where the wall shear stress balances gravity and the film thickness is uniform. In this case the upper limit of the integrals in Eq. (35) can be the length of the curved zone. This means that the mixing pressure drop ΔP_{mix} equals the sum of the gravitational and the wall shear stress contribution in the liquid film adjacent to the curved nose of the bubble. This observation was first pointed out by Barnea (1989) for the vertical case and Taitel and Barnea (1989) for the inclined case and it has some interesting consequences when the approximation of uniform equilibrium liquid level is used.

When the simplified approach, which considers the liquid film in constant equilibrium thickness, is used (Fernandes *et al.*, 1983; Sylvester, 1987), the calculation of the pressure drop via Eqs. (25) and (27) is not consistent and yields different results. Equation (25) in this case reads

$$\Delta P_u = \rho_s g\sin\beta l_s + \frac{\tau_s \pi D}{A} l_s + \rho_f g\sin\beta l_f + \frac{\tau_f S_f}{A} l_f + \frac{\tau_G S_G}{A} l_f \tag{36}$$

where $\rho_f = \alpha_f \rho_G + R_f \rho_L$.

Note that in the film zone, gravity is balanced by the shear forces. Assuming now that the pressure drop in the gas bubble is negligible [this is the same assumption that was used in deriving Eq. (27)], this leaves only the first two terms in Eq. (36). This result is clearly in contradiction to Eq. (27), where ΔP_{mix} is given by the conventional acceleration term [Eq. (29)]. As pointed out by Barnea (1989) and demonstrated by Eq. (35), one has to consider a curved nose in order to obtain the same results for the pressure drop by using either Eq. (25) or (27).

Barnea (1989) compared the results of the pressure drop for the constant film thickness model with the more exact solutions. She showed that for the vertical case, when a cylindrical bubble with a flat nose is assumed, the results of the pressure drop, without the acceleration term [in Eq. (27)], is usually closer to the more exact solution than when the acceleration term is used. Note that in the work of Fernandes *et al.* (1983)) and Sylvester (1987), the acceleration term was considered, although the constant film thickness approximation was used.

E. Auxiliary Relations

The formulations provided so far are not sufficient yet to obtain a solution. In order to proceed, we should consider the following additional variables: (1) the translational velocity u_t, (2) the dispersed bubbles velocity u_b, (3) the liquid holdup in the liquid slug zone R_s, and (4) the liquid slug length l_s or the slug frequency ν_s. We will term these variables as auxiliary variables. It is convenient for the time being to consider them as

k. w v. .a. .s, gi\ n ... t..m. of known formulas, and postpone the discussion on determining their values to the end of the chapter. In this manner the solution procedure can be presented in a more general manner. Namely, a solution can be performed for any of these values regardless of the details of their correlations.

The translational velocities are the velocities of the interfaces and this applies, in principle, both to the elongated bubble in the film zone (Taylor bubble in the vertical case) as well as the dispersed bubbles within the liquid slug zone. As mentioned, the translational velocity of the elongated bubble u_t is larger than the gas velocity within this bubble u_G. The prediction of this translational velocity is not an easy task and, in fact, it is the subject of current research. It is assumed, however, that the translational velocity can be expressed as a linear relation of the slug mixture velocity as

$$u_t = Cu_s + u_d \tag{37}$$

where u_d is the drift velocity, namely, the velocity of propagation of a large bubble in stagnant liquid and the factor C is related to the contribution of the mixture velocity. This factor is larger than unity as it is influenced by the liquid velocity profile ahead of the bubble. This expression is very similar to the Zuber and Findlay (1965) distribution parameter, although here it results from an entirely different reason. C and u_d are both considered constant for given operation conditions and, in fact, they are usually taken as constants for all flow conditions. At the present time we will assume that both C and u_d are known. A special discussion will be given later on the methods used to find these values.

The dispersed bubbles translational velocity can be expressed in a similar manner:

$$u_b = Bu_s + u_0 \tag{38}$$

However, unlike the case of the elongated (Taylor) bubbles, the translational velocity and the gas velocity are the same for the small bubbles. The coefficient B is the distribution parameter and u_0 is the drift velocity for stagnant liquid. A discussion for the recommended values of B and u_0 will be presented later.

The liquid holdup within the liquid slug zone R_s depends on the flow rates of the liquid and the gas and the pipe inclination. The relation for R_s is obtained either from experimental correlations or by a mechanistic model.

Finally information for the liquid slug length or slug frequency should be given. The liquid slug length and the slug frequency are interrelated variables and it is sufficient if one of these values is given.

As mentioned, we will assume that these four variables are known and proceed towards a solution. Later, a special discussion will follow and the state of the art for determining these variables will be presented.

F. Calculation Procedure

The set of equations obtained so far (including the auxiliary relations) allows the calculation of the detailed slug structure, which is the basis for calculating the pressure drop as well as heat and mass transfer. A solution is sought for a given set of operating conditions, namely, liquid and gas flow rates, pipe diameter and inclination, as well as the physical properties of the liquid and the gas. As demonstrated in a previous section, the calculation of the average void fraction α_u can be performed immediately using Eq. (8) or (9), which are independent of the detailed slug structure.

Unfortunately the detailed slug structure as well as the pressure drop calculations is not that simple and it requires some numerical efforts. The complexity of the calculations depends largely on the way the shape of the liquid film is calculated. We have distinguished three basic cases as related to the method used for calculating the hydrodynamic of the liquid film (see Section II,C): (1) accurate film profile, (2) simplified film profile (τ_i, $\tau_G = 0$), and (3) constant equilibrium level.

For convenience, we shall start with the simplest case, case 3, where an equilibrium constant liquid level (or constant film thickness) is assumed. This method was used primarily for vertical slug flow (Fernandes *et al.*, 1983; Orell and Rembrand, 1986), while for the horizontal case, both Dukler and Hubbard (1975) and Nicholson *et al.* (1978) considered the shape of the liquid film. In principle there is no reason why the constant equilibrium level was adopted only for the vertical case and not for the horizontal case. A partial justification for it is that in the vertical case the liquid film reaches an equilibrium thickness in a shorter distance than in the horizontal case. Yet this situation depends largely on the flow rates of the liquid and gas.

The solution in this case first requires the calculation of the terminal equilibrium level h_E (or δ_E). This is done via an implicit solution of Eq. (24) for the film thickness. The calculation sequence can be visualized as a trial-and-error procedure as follows:

1. u_s is calculated using Eq. (6) (the superficial velocities are assumed to be known).
2. The auxiliary variables u_t, u_b, R_s, and l_s are determined first; u_t is calculated using Eq. (37); u_b is calculated using Eq. (38); R_s and l_s are also evaluated by the proper methods (Sections II,I. and II,J.).
3. u_L is determined using Eq. (6).

4. A first guess for h_f is assumed, which allows for the calculation of the geometrical parameters A_f, R_f, A_G, S_f, S_G, and S_i. For a stratified film, the following geometrical relations are used:

$$R_f = (1/\pi)\{\pi - \cos^{-1}[2(h_f/D) - 1] + [2(h_f/D) - 1]\sqrt{1 - [2(h_f/D) - 1]^2}\} \tag{39}$$

$$S_f = D\{\pi - \cos^{-1}[2(h_f/D) - 1]\} \tag{40}$$

$$S_i = D\sqrt{1 - [2(h_f/D) - 1]^2} \tag{41}$$

For a symmetrical annular film, simpler geometrical relations can be readily obtained.

5. u_f is extracted from Eq. (4).

6. u_G can be calculated using a mass balance on a cross section in the film zone [similar to Eq. (6)]:

$$u_G\alpha_f + u_fR_f = u_s \tag{42}$$

7. The friction factors f_f, f_G, and f_i are evaluated on the basis of the appropriate Reynolds number. For this purpose there are a few options as discussed earlier. For example, one may use Eq. (16) for f_f and f_G and a constant value for f_i (see Cohen and Hanratty, 1968, for stratified flow) or Eq. (17) for annular flow.

8. The shear stresses τ_f, τ_G, and τ_i are calculated using Eqs. (12)–(14).

9. At this point, all the variables in Eq. (24) can be calculated, and one can check whether the trial film thickness is correct. Obviously, the approach for obtaining the correct solution h_f is to use one of the standard methods to ensure fast convergence such as the interval bisection method, the method of false position, Newton–Raphson method, or any other appropriate method.

10. Since slug length l_s is considered known, the film length can now be calculated using Eq. (2) for the unknown l_u. This results in

$$l_u = l_s(u_LR_s - u_fR_f)/(u_{LS} - u_fR_f) \tag{43}$$

It should also be mentioned that under most conditions τ_G and τ_i are very small and can be neglected as was indeed the case in most of the previous reported works. This simplification, however, saves only minor computational efforts and is not recommended for the general case since it can cause a serious error for the case where very long elongated bubbles exist.

Once the film thickness is known, one can proceed and calculate the pressure drop. For this purpose one can use either Eq. (25) or (27). Both, in principle, should give the same results. However, due to the approximation taken here and the neglect of the curved shape of the bubble nose, Eq. (25) is not consistent with Eq. (27). This point was discussed in detail by Barnea (1989) and Taitel and Barnea (1989). For vertical upward flow, Barnea (1989) showed that in the case of an uniform film thickness, Eq. (25) will somewhat underpredict the pressure drop, whereas Eq. (27) will overpredict the pressure drop, comparing it to the case where the bubble shape is taken into account. However, Eq. (25) is usually much closer to the more exact solution. Thus, when using the constant-film-thickness approach it is recommended to use Eq. (25) rather than Eq. (27), namely, to ignore the acceleration term in the pressure calculation. This is contrary to the way Fernandes *et al.* (1983) made their calculation (for the vertical case) and is consistent with the Orell and Rembrand (1986) calculations. For the horizontal case, both Dukler and Hubbard (1975) and Nicholson *et al.* (1978) used Eq. (27). Since they did not neglect the curved nose their method of calculation should have yielded the same result as Eq. (25). However, as pointed out by Taitel and Barnea (1989), they calculated the pressure drop in the mixing zone erroneously, neglecting the integral terms on the right-hand side of Eq. (30), which may result in a serious error for large-diameter pipes.

The term *accurate film profile* (case 1) is used when the exact Eq. (21) is used to integrate the liquid film level $h_f(z)$. The *simplified film profile* (case 2) is used when the pressure drop in the film zone is neglected, and $h_f(z)$ is obtained via the integration of Eq. (23), instead of Eq. (21). Both cases, however, require numerical integration and their solution is very similar. The solution follows the following steps:

1. The variables u_f, u_s, R_s, u_b, and u_L are calculated as in case 3.
2. h_s is calculated, using Eq. (39) on the basis of the value of R_s.
3. The critical level h_c is calculated by finding the level at which the denominator in Eq. (21) equals zero.
4. The value of h_f at $z = 0$, h_{fi}, is set equal to the lower value of h_s or h_c.
5. Equation (21) or (23) (for case 2) is integrated numerically to yield $h_f(z)$. This integration is carried out until the mass balance [Eq. (5)] is satisfied and, thus, the film zone length is obtained. Note that Dukler and Hubbard (1975) as well as Nicholson *et al.* (1978) applied the integration only to the approximate Eq. (23). Also their method of integration was different. Instead of integrating $h_f(z)$ (or R_f), they integrated $z(R_f)$.

As mentioned, cases 1 and 2 will usually yield similar results. However, for the case of very long film zones, the pressure drop in the gas cannot be neglected. Since the efforts in the calculation of case 2 are not much easier than in the general case (case 1), it is recommended to use the exact method (case 1) for all the calculations.

6. Since the numerical integration provides the profile of all the variables in the film zone, the pressure drop can be easily obtained using Eq. (25) or (27) (when the pressure drop in the gas zone is ignored). If Eq. (27) is used, the pressure drop in the mixing zone can be calculated by either Eq. (30) or (35).

All in all, the calculation procedure describes a considerable number of options for the user. It is not written in a "ready to use" single format and the results are not presented in the form of a computer program or exact flow chart. It leaves some effort to the user to choose the option appropriate for his specific use and to write his own program. It does, however, contain sufficient details to guide the reader in the use of the options available and present the advantages and drawbacks of the various possibilities.

G. Translational Velocities of Elongated (Taylor) Bubbles

As discussed earlier, Eq. (37) was assumed to apply for the translational velocities, and the constants C and u_d were assumed to be known. We will discuss now the methods by which these variables are determined.

The idea behind the specific form of Eq. (37) is that the translational velocity can be composed as a superposition of the velocity of bubbles in a stagnant liquid (or liquid mixture) u_d and the additional contribution of the mixture velocity u_s. Also it is assumed that the translational velocity is linearly dependent on the mixture slug velocity. Obviously these assumptions are just an approximation, subject to experimental and theoretical verification.

The motion of elongated bubbles is usually treated separately for the vertical case (Marrucci, 1966; Bendiksen, 1985; Nicklin, 1962; Nicklin *et al.*, 1962; Davies and Taylor, 1949; Dumitrescu, 1943), the horizontal case (Kouba, 1986; Nicholson *et al.*, 1978; Dukler and Hubbard, 1975), and the more general upward inclined case (Stanislav *et al.*, 1986; Hasan and Kabir, 1986; Zukoski, 1966; Singh and Griffith, 1970; Bendiksen, 1984.) The first attempt, and the most successful one, was the treatment of the vertical case in which reasonable agreement among different researchers exists and both empirical correlations and theoretical approaches seem to be satisfactory. For the horizontal case the situation is less clear. For example, Wallis (1969), Dukler and Hubbard (1975), as well as Bonnecaze *et al.* (1971) claimed that the drift velocity is zero for the horizontal case since the buoyancy force does not act in the flow direction. Only later Nicholson *et al.* (1978), Bendiksen (1984), and others showed that a drift velocity exists also for the horizontal case and, in fact, it may even exceed its value in the vertical case (Weber, 1981).

The drift velocity depends on the detailed two-dimensional flow at the front of the bubble. Note that the simple one-dimensional approach based on channel flow approximation is not suitable for analyzing the immediate region of the bubble nose. Fortunately, approximations that are based on potential flow yield reasonable results. Davies and Taylor (1949) were first to perform such a calculation for the vertical case. Their first approach was quite simple. They consider a potential flow around the nose of the bubble:

$$q^2 = U^2 \tfrac{9}{4} \sin^2 \theta \tag{44}$$

where q is the tangential liquid velocity on the surface, θ is a polar coordinate, and U is the free-stream velocity.

Application of the Bernoulli equation and considering the pressure within the bubble as constant yields that $gz = q^2/2$. Substituting this relation in Eq. (44) yields for small θ:

$$U = u_d = (2/3\sqrt{2})\sqrt{gD} = 0.471\sqrt{gD} \tag{45}$$

In Eq. (45) D is the bubble diameter. Modification of this equation, which takes into account the bubble rise in a confined pipe, was also performed by Davies and Taylor (1949). They used a series expansion technique and obtained the same form of Eq. (45) with a constant of 0.328 instead of 0.471. Dumitrescu (1943) performed somewhat more accurate calculations and obtained the constant of 0.35, which thereafter was accepted as the best value that also agrees very well with experimental observations (Nicklin *et al*, 1962).

For the horizontal case the situation is less clear. The most interesting fact is that some of the papers do use the drift velocity, whereas others consider the drift velocity as zero on the basis that gravity cannot act in the horizontal direction. The more recent work of Nicholson *et al.* (1978), Weber (1981), Bendiksen (1984), and Kouba (1986) clearly show that a drift velocity exists also for the horizontal case owing to gravity-induced drift that results from elevation difference in the bubble nose.

Consistent with the approach taken for the vertical case, in the horizontal case also the inviscid theory is applied near the nose region. The drift velocity in horizontal slug flow is the same as the velocity of the penetration of a bubble when liquid is emptied from a horizontal tube (Benjamin, 1968). To predict this velocity the following relations are considered (see Fig. 2):

Continuity:

$$Av_1 = A_2 v_2 \tag{46}$$

where A_2 is given by

$$A_2 = (\pi - \gamma + \tfrac{1}{2}\sin 2\gamma) r^2 \tag{47}$$

Bernoulli theorem is applied between point (1) and the stagnation point (0). Note that the pressure at the stagnation point, which is the same as

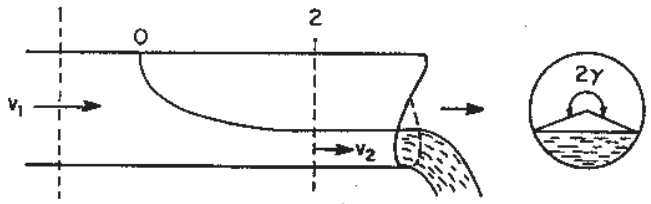

FIG. 2. Propagation of gas pocket in the draining horizontal pipe.

the pressure in the gas bubble, is taken as the reference pressure:

$$P_1 = -\tfrac{1}{2}\rho v_1^2 \tag{48}$$

Bernoulli theorem between points (0) and (2) along the free surface yields

$$v_2^2 = 2gr(1 - \cos\gamma) \tag{49}$$

Finally a momentum balance yields

$$(P_1 + \rho g r)\pi r^2 - \int_0^h \rho g(h - y)b\, dy = \rho v_2 A_2 (v_2 - v_1) \tag{50}$$

where the integral term in Eq. (50) can be solved explicitly, namely,

$$\int_0^h \rho g(h - y)b\, dy = \rho g r\left(A_2 \cos\gamma + \frac{2}{3} r^2 \sin^3\gamma\right) \tag{51}$$

As shown in Benjamin (1968), Eqs. (46)–(50) are solved for the liquid level h_2 (equivalent to A_2 or γ) and the liquid velocities v_1 and v_2. The results are

$$h_2/D = 0.563 \qquad \text{and} \qquad v_1 = u_d = 0.542\sqrt{gD} \tag{52}$$

The result of Eq. (52) is supported experimentally (for bubbles with a negligible effect of surface tension) by Zukoski (1966) and Bendiksen (1984). It is interesting to observe that the drift velocity in the horizontal case is larger than the drift velocity in the vertical case.

For the inclined case, there is no proposed model and one relies primarily on experimental data. The inclined case, as well as the vertical and the horizontal cases, were studied by Zukoski (1966), Singh and Griffith (1970), Bonnecaze *et al.* (1971), Bendiksen (1984), and Hasan and Kabir (1986). All report a peculiar behavior, that the drift velocity increases as the angle of inclination is declined from the vertical position. The drift velocity then decreases again toward the horizontal position such that the maximum drift velocity occurs at an intermediate angle of inclination

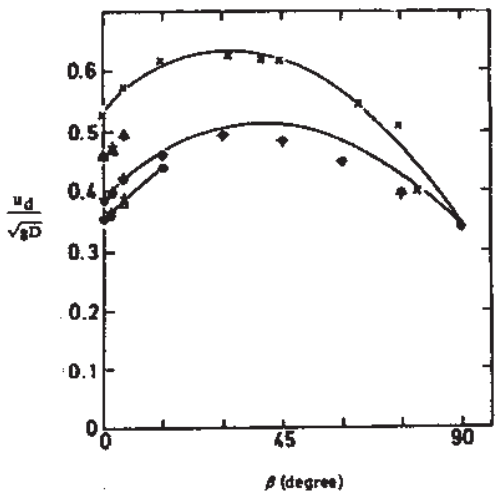

FIG. 3. Dimensionless bubble velocity in stagnant liquid versus inclination angle for different surface tension parameters: (——) predicted; (□) $\Sigma = 0.064$; (○) $\Sigma = 0.042$; (△) $\Sigma = 0.01$; [Bendiksen, 1984] (×) $\Sigma = 0.001$; (+) $\Sigma = 0.01$, 0.042, 0.064 [Zukoski, 1966] (after Bendiksen, 1984).

around 40° to 60° from the horizontal. Bonnecaze *et al.* (1971) were the first to give a qualitative explanation for this peculiar behavior, arguing that the gravitational potential that drives the liquid velocity along the curved surface at the bubble nose increases and then decreases as the angle of inclination changes from the vertical position towards the horizontal position.

Figure 3 shows the results of Bendiksen (1984) and Zukoski (1966) for the change of the dimensionless drift velocity $u_d/\sqrt{gD}$ with the angle of inclination. The upper curve represents the case where surface tension is negligible and, thus, the results for the horizontal and the vertical limits very closely follow the aforementioned theoretical results that were based on potential flow; namely, that $u_d/\sqrt{gD} \simeq 0.35$ for the vertical case ($\beta = 90°$) and $u_d/\sqrt{gD} \simeq 0.54$ for the horizontal case. The surface tension effect is given in terms of the surface tension parameter $\Sigma = 4\sigma/g(\rho_L - \rho_G)D^2$. Figure 4 shows the experimental data reported by Zukoski (1966). It shows that the effect of surface tension can indeed be substantial, particularly for small-diameter pipes. For a small surface tension parameter $\Sigma \simeq 0.001$, the results for the vertical case and the horizontal case are very close to the potential flow theory, namely, $u_d/\sqrt{gD} \simeq 0.35$ and 0.54, respectively. The drift velocity, however, decreases considerably with an increase in the surface tension parameter (decreasing the pipe diameter) and eventually reaches a zero velocity when Σ is of the order of unity.

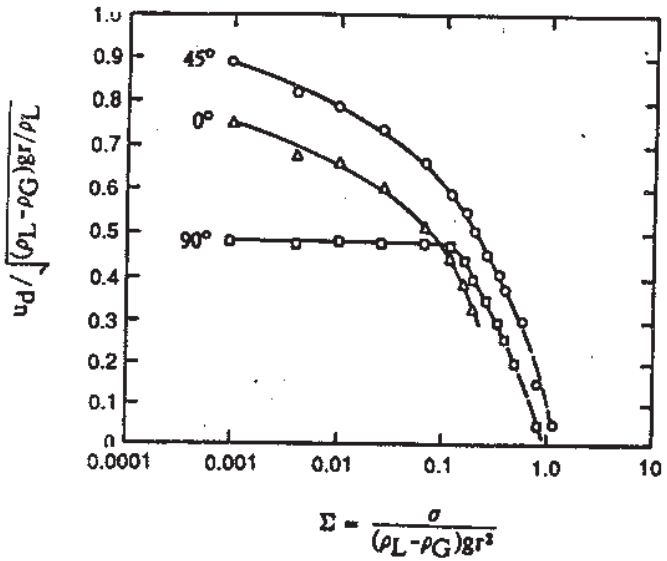

FIG. 4. Variation of normalized velocity with surface tension parameter for $\beta = 0°$, 45°, and 90° (after Zukoski, 1966).

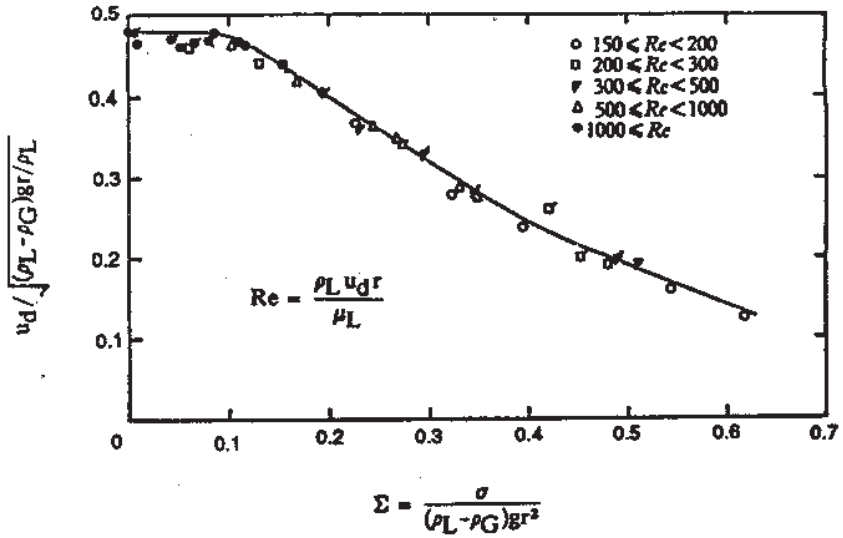

FIG. 5. Bubble velocity versus surface tension parameter for ranges of Reynolds numbers. Flagged symbols from Barr (1926), Dumitrescu (1943), and Goldsmith and Mason (1962) (after Zukoski, 1966).

The drift velocity is expected to depend also on the liquid viscosity, or the bubble Reynolds number. However, Zukoski (1966) shows that the dependence of the drift velocity on viscosity is negligible for Reynolds number $\mathrm{Re} > 300$ ($\mathrm{Re} = u_d \rho_L D/\mu_L$). This is clearly demonstrated by Fig. 5.

Bendiksen proposed, as a practical suggestion, to use the following formula for the drift velocity in the inclined case:

$$u_d = u_d^h \cos\beta + u_d^v \sin\beta \tag{53}$$

where u_d^h and u_d^v correspond to the drift velocity for the horizontal and the vertical case, respectively.

Hasan and Kabir (1986) proposed the relation:

$$u_d = u_d^v \sqrt{\sin\beta}(1+\cos\beta)^{1.2} \tag{54}$$

which they claim to well correlate experimental data in the range $90° > \beta > 30°$.

Next we will consider the additional contribution of the mixture velocity to the elongated bubbles translational velocity, namely, the value of the constant C on the right-hand side of Eq. (37). In developed slug flow, the translational velocity is usually related to the value of the liquid slug velocity at the centerline, where the velocity attains its maximum. This is based on the assumption that the propagation velocity of the bubbles is equal to the maximum local liquid velocity in front of the nose tip (Nicklin *et al.*, 1962; Nicklin, 1962; Collins *et al.*, 1978; Bendiksen, 1984, 1985; Shemer and Barnea, 1987). Although this is a rather simplified approach, it has been found remarkably valid and supported by the more exact approaches (Collins *et al.*, 1978) and by experimental data. Thus for turbulent flow, $C \simeq 1.2$, which is the ratio of u_{max}/u_{mean} for turbulent flow. Nicklin *et al.* (1962) state that this value is valid for a Reynolds number greater than 8000 but it is also a good approximation for a Reynolds number less than that. For laminar flow the ratio u_{max}/u_{mean} approaches 2 and indeed there is a strong indication that C increases as the Reynolds number decreases and reaches a value of about 2. A more precise theory shows that C, for laminar flow, equals 2.27 (Taylor, 1961; Collins *et al.*, 1978) for the case where the surface tension is neglected. Experimental results that were carried out at about $\Sigma = 0.05$ show that C is 1.87 (Collins *et al.*, 1978), 1.94 (Bendiksen, 1985), and 1.8 to 1.95 (Nicklin *et al.*, 1962). Figure 6 is an example of Bendiksen (1985) data on the effect of Reynolds number on the coefficient C. As seen, C has the value of about 1.2 at a high

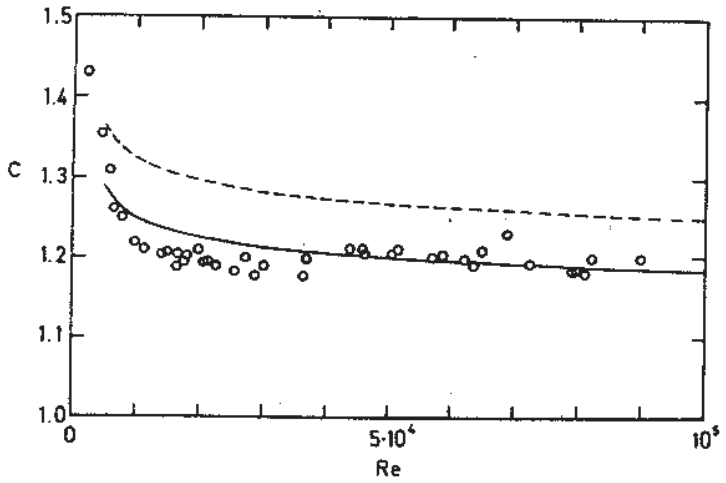

FIG. 6. A comparison of predicted and measured distribution slip parameters C (O) $\Sigma = 0.042$ [data of Bendiksen (1984)]; (——) predicted with $\Sigma = 0.042$; (- - - -) predicted with $\Sigma = 0$ (after Bendiksen, 1985).

Reynolds number and it increases as the Reynolds number decreases. The limit of about $C = 2$ is not shown in this figure.

The exact value of C for the turbulent case, and in particular for the laminar case, is not conclusive. There is still a spread in the experimental data as well as the various theories. Yet, at least to a good engineering approximation, the values of $C = 1.2$ for turbulent flow and $C = 2$ for laminar flow is quite a good approximation for the case where the effect of surface tension is small. Furthermore, it is applicable both for the vertical case, the horizontal case, and also the inclined case (Bendiksen, 1984).

It should be stressed that the theoretical consideration just presented is consistent with the assumption that the translational velocity is a linear function of the mixture (slug) velocity as expressed by Eq. (37). Although this is a valid engineering approximation, it is not necessarily the exact representation of the real situation. If one plots experimental data of u_t versus u_s and extrapolates to $u_s = 0$, obviously the result for $u_s = 0$ is the drift velocity. If the curve u_t versus u_s is not quite a straight line (which is the realistic case), then one has several options. One can draw a straight line that originates at the point $u_s = 0$, $u_t = u_d$, and draw a best fit over the range form $u_s = 0$ up to any desired value. Another option is to fit a straight line over any desired interval where u_s is larger than zero. In this case u_d is the extrapolation of this straight line to the zero point and it would not be the same as the mentioned drift velocity. Bendiksen (1984) showed that in this case the value of u_d is usually less than the one reported here due to the fact that the u_t versus u_s curve bends slightly upwards. However, it seems to us that for any practical application a straight line that originates from the point $(0, u_d)$ is adequate for the accuracy needed for engineering calculations.

H. Velocities of the Dispersed Bubbles in the Liquid Slug

A rough criterion to distinguish between the elongated (Taylor) bubbles and the dispersed bubbles within the liquid slug is the characteristic value of the pipe diameter. Bubbles with a chord length larger than the pipe diameter D are considered elongated bubbles. Smaller bubbles are usually termed as dispersed bubbles.

As in the case of the translational velocity for elongated bubbles, it is assumed that the velocity of the bubbles in the liquid slug u_b is a linear combination of the bubble drift velocity u_0 and the mixture velocity in the slug zone u_s, as it is reflected by the form of Eq. (38). In Eq. (38), B is the distribution parameter (Zuber and Findlay, 1965) and u_0 is the drift velocity.

For the vertical case the drift velocity is the free-rise velocity of a bubble in the pipeline. This free rise can be evaluated by considering the free-rise velocity of a single bubble in an infinite medium, the free rise of a bubble in a swarm of bubbles (the effect of voids in the liquid slug), and finally the free-rise velocity in a cylindrical pipe. This subject has been discussed extensively (see e.g., Brodkey, 1967; Levich, 1962; Govier and Aziz, 1972; Wallis, 1969).

The free-rise velocity of a single bubble in an infinite media depends largely on the size of the bubble. For very small bubbles the bubbles behave as rigid spheres and the free rise is governed by Stokes law. For larger bubbles, a boundary-layer solution is applicable. As the bubble diameter increases, circulation effects take place and affects the free rise. When the bubbles become larger, their spherical shape is distorted and flattens. This has a drastic effect on slowing down the free rise compared to an equivalent spherical bubble. When the bubble size exceeds some critical value, the rise velocity of the dispersed bubble tends to be constant and independent of the bubble diameter. This critical bubble size is (Brodkey, 1967)

$$d_{crit} = [0.4\sigma/(\rho_L - \rho_G)g]^{1/2} \tag{55}$$

The bubbles in the liquid slug zone are usually larger than d_{crit}. For a relatively large and deformable bubble, the equation proposed by Harmathy (1960) for the bubble rise velocity is considered of sufficient accuracy:

$$u_\infty = 1.54[\sigma g(\rho_L - \rho_G)/\rho_L^2]^{1/4} \tag{56}$$

Note that Eq. (56) indeed shows that the free-rise velocity is independent of the bubble size.

The free-rise velocity of a bubble within a swarm of bubbles is lower than the free rise of a single bubble. This can be viewed as the decrease of buoyancy that acts on a single bubble in a gas–liquid mixture. This decrease is correlated in the form

$$u_0 = u_\infty(1 - \alpha_s)^n \tag{57}$$

For relatively large bubbles, Wallis (1969) as well as Govier and Aziz (1972) suggested the use of $n = 1.5$. Fernandes *et al.* (1983) used $n = 0.5$. A value of $n = 0$ was recommended by Wallis (1969) (after Zuber and Hench, 1962) for the region termed as churn turbulent. The later case is probably most close to the flow of bubbles in the slug region and, thus, the value $n = 0$ is suggested. It should be noted that no direct information is available on the rise velocity of bubbles within the liquid slug. However, for modeling slug flow, the accuracy of the rise velocity is usually not that important anyway.

Finite size of the pipe also acts to decrease the free-rise velocity. This effect is discussed by Wallis (1969). In general, the effect of the pipe diameter is negligible for $d/D < 0.125$, and it is suggested to ignore it.

For the case of inclined pipes, we may assume that the drift velocity u_0 should be multiplied by $\sin\beta$ (Barnea *et al.*, 1985).

The value of B depends on the concentration distribution of the bubbles in the liquid slug as demonstrated by the method of Zuber and Findlay (1965). Wallis (1969) points out that B for vertical dispersed flow "usually lies between 1.0 and 1.5 with a most probable value of about 1.2." For the horizontal case the bubble concentration is definitely not uniform since bubbles tend to concentrate at the top of the pipe. Nevertheless B was taken as unity since it was assumed that the dispersed bubbles have the same average velocity as the liquid in the mixture. Kouba (1986) did measure the distribution parameter in horizontal slug flow and got a value close to 1.2. However, owing to the lack of supporting evidence we would recommend the use of $B = 1$ for the horizontal case. As can be seen the evaluation of B for horizontal, vertical, as well as the inclined case is still an open question.

I. Liquid Holdup in the Liquid Slug Zone

As indicated in Section II,E, the model calculations require as input data the value of the liquid holdup within the liquid slug R_s. This value may be obtained experimentally or through a physical model.

Hubbard (1965) measured R_s in an air–water horizontal slug system by using an impact Pitot probe system. This technique proved to be very difficult for realization. Considerable scatter was observed and the results obtained showed little consistency.

Experimental values of R_s, using a light refined oil–air system in a horizontal pipe, were obtained by Gregory *et al.* (1978). They used capacitance-type liquid-volume-fraction sensors, which provided a continuous record of the *in situ* liquid volume fraction. The ranges of flow rates investigated cover virtually the entire region of slug flow that was observed in their flow loop. For air–oil slug flow in horizontal 2.58- and 5.12-cm I.D. pipes, they found a modest diameter effect and suggested a correlation of the following form:

$$R_s = \frac{1}{1 + (u_s/8.66)^{1.39}} \tag{58}$$

where the mixture velocity u_s has units of meters per second.

In spite of the fact that this correlation is limited and does not include the effect of fluid properties and pipe diameter, it is frequently used because of its simplicity.

Greskovich and Shrier (1971) presented a graphical correlation of R_s involving the mixture Froude number (u_s/Dg) and the input liquid quality (λ). This correlation is based on data collected with air–water in a 1.5-cm I.D. horizontal pipe. Values of R_s between 1 and 0.5 were obtained.

Heywood and Richardson (1979) used the γ-ray absorption method in order to determine the average holdup within the liquid slug for an air–water system in a 4.2-cm horizontal pipeline. The results are presented by a graphical correlation of R_s versus u_{GS} with parametric values of u_{LS}. These results are similar to the correlation presented by Gregory *et al.* (1978).

Schmidt (1977) measured the liquid holdup in the liquid slug in vertical risers by using a capacitance sensor. Void fraction in the liquid slug was correlated with u_{LS} and u_{GS}. The values of the void fraction range from 0.2 to 0.8.

Fernandes (1981) measured R_s in a vertical air–water slug flow using a 5-cm I.D. pipe. Based on his experimental results, he suggested that R_s be set equal to 0.25. It should be mentioned that Fernandes' data was obtained for a relatively limited u_{GS}–u_{LS} range.

Barnea and Brauner (1985) proposed a method for estimating the gas holdup within the liquid slug, α_s. It was suggested that the gas holdup on the transition line from dispersed bubbles is the maximum holdup that the liquid slug can accommodate as fully dispersed bubbles at a given mixture velocity u_s. Thus, curves of constant u_s within the intermittent region represent the locus where α_s or R_s is constant and is equal to the holdup of the dispersed bubble pattern at the transition boundary. The transition boundary itself may be obtained by any reliable predictive model or experimentally. Once it is obtained, R_s may be determined by the previously mentioned concept. For example, using the theoretical transition boundary from dispersed bubbles for the vertical case, yields (Barnea, 1987),

$$\alpha_s = 1 - R_s = 0.058\{2[0.4\sigma/(\rho_L - \rho_G)g]^{1/2}[(2f_s/D)u_s^3]^{2/5}(\rho_L/\sigma)^{3/5} - 0.725\}^2 \quad (59)$$

Note that Eq. (59) usually applies also to the inclined and horizontal cases (see Barnea, 1987, for possible exceptions).

The calculated value of R_s ranges from 1 to 0.48, where 0.48 is associated with the maximum volumetric packing of the dispersed bubbles in the liquid slug. For the special case of vertical and off-vertical pipes with relatively large diameters ($D > 0.05$ m for air–water), the maximum value of R_s is 0.75 (Barnea and Brauner, 1985).

Barnea and Shemer (1989) used a conductance probe to detect the instantaneous void fraction at the centerline of a vertical 0.05- m I.D. tube in upward air–water slug flow. This information was further processed to obtain the liquid slug holdup and its length. The experimental values of voidage ranges from $\alpha_s = 0.25$ on the transition from bubbly flow, to $\alpha_s = 0.6$ near the transition to churn flow, as has been predicted by Barnea and Brauner (1985).

J. Slug Length and Slug Frequency

The slug frequency and the liquid slug length are interconnected properties and are very often alternatively used (Nicholson *et al.*, 1978). Experimental observations for air–water systems in vertical upward and horizontal slug flows suggest that the stable liquid slug length l_s is relatively insensitive to the gas and liquid flow rates and is fairly constant for a given tube diameter. The stable slug length has been observed to be of about $12–30D$ for horizontal slugs (Dukler and Hubbard 1975). Nicholson *et al.* (1978) noted that the variations in the average liquid slug length are much smaller than the corresponding slug unit length and reported an average value of $30D$. For the vertical case the observed liquid slug length is about $10–20D$ (Moissis and Griffith, 1962; Moissis, 1963; Akagawa and Sakaguchi, 1966; Fernandes, 1981; Barnea and Shemer, 1989).

Slug frequency has sometimes been considered as an entrance phenomenon, namely, it results from bridging of the liquid at the entrance (Taitel and Dukler, 1977). This is indeed the case in horizontal and slightly inclined flows, near the transition from stratified flow. In this case low-frequency slugs are generated causing relatively long liquid slugs at the entrance which propagates downstream. However, generally short (high frequency) slugs are formed at the entrance of the pipe. These slugs are usually unstable. Shedding of liquid at the rear of the liquid slug seems to be larger for short slugs. As a result, an elongated bubble behind a short slug moves faster and overtakes the bubble ahead of it (Moissis and Griffith, 1962). The bubble and the corresponding liquid slug merge in this process, decreasing the slug frequency. The merging process continues until the liquid slug is long enough to be stable, namely, the trailing bubble is unaffected by the wake of the leading one. This occurs when the velocity profile at the rear of the liquid slug can be considered fully developed (Moissis and Griffith, 1962; Taitel *et al.*, 1980; Barnea and Brauner, 1985; Dukler *et al.*, 1985).

Taitel *et al.* (1980) and Barnea and Brauner (1985) simulated the mixing process between the film and the slug by a wall jet entering a large reservoir. The process of establishing the stable slug length can be visualized as follows. Referring to Fig. 7, two consequent elongated bubbles are shown. The first is behind a long steady liquid slug. The velocity profiles within this slug are shown as they develop from a mixing wall jet profile to a fully developed pipe flow at the back of the slug. Since the average total mixture velocity at any cross section of the slug is the same and equals u_s, it is obvious that the maximum velocity decreases asymptotically towards the value of $1.2u_s$ with distance from the front of the liquid slug. As the bubble velocity is related to the local maximum velocity ahead of it, it is clear that bubble B, which is behind a short liquid slug is faster than bubble A, which is behind a fully developed profile with $u_{max} = 1.2u_s$. Thus, bubble B will overtake the leading bubble A. This is the process by which short slugs tend to disappear. This process however is terminated once all the slugs are

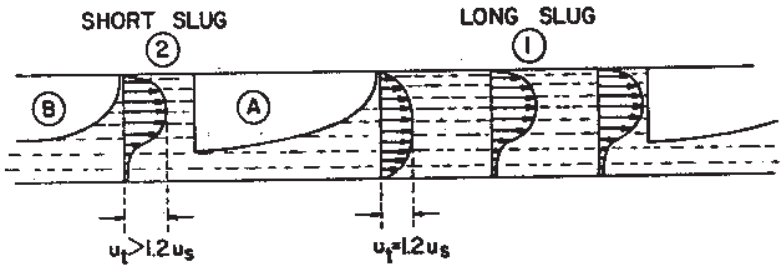

Fig. 7. Velocity profiles in liquid slugs.

long enough so that the velocity profile at the back of the slugs is fully developed. Thus, this process is usually the one that controls the slug length. Taitel *et al.* (1980) and Barnea and Brauner (1985) suggested that a developed slug length is equal to a distance at which a jet has been absorbed by the liquid. Using this approach, a value of $16D$ was obtained for the minimum liquid slug length in vertical upflow and a value of $32D$ was obtained for the case of horizontal flow.

Dukler *et al.* (1985), on the other hand, assumed that the liquid at the front of the slug is well mixed with an uniform velocity profile. From this point on, a boundary layer is developed at the pipe wall until a fully developed velocity profile is achieved. They found that the minimum stable slug length l_s is of the order of $20D$. Although the final results of Dukler *et al.* are similar to the previous analysis, it does not explain well the merging mechanism. In their approach, the value of the centerline velocity increased with the distance from the liquid slug front, and the maximum velocity, which determines the bubble velocity, is minimal behind short slugs. Namely, elongated bubbles behind short liquid slugs will move slower then those behind longer ones, contrary to experimental observation.

Shemer and Barnea (1987) used the hydrogen-bubble technique to record the velocity profiles behind the elongated bubbles in gas–liquid slug flow. They distinguished between two zones in the development of the velocity profile. The first zone is an annular jet, which terminates at a distance of about 2–$3D$, causing a strongly disturbed velocity profile in the whole cross section of the pipe. At larger distances from the bubble, a gradual decay of the fluctuations occurs until a fully developed profile is obtained. Shemer and Barnea (1987) found that the bubble shape in the wake region closely resembles the liquid velocity profile ahead of it. They, thus, concluded that the propagation velocity of the elongated bubble is related to the maximum instantaneous liquid velocity ahead of it. They found a steep decrease in this maximum velocity in the near-wake region, while a much more gradual decrease is observed at larger distances from the leading bubble until a fully developed velocity profile is observed. In this case the lowest possible value of the instantaneous maximum value is obtained. This distance from the leading bubble determines the minimum length of the stable liquid slugs where all the bubbles have a smooth rounded front shape and propagate with identical velocity. The detected velocity field in the wake of the bubble was utilized by the investigators to estimate the minimum stable slug length. They found that l_s is of the order of $20D$.

Most of the reported data and correlations on slug frequency and slug length are related to the downstream developed slugs and not to the entrance frequency.

Gregory and Scott (1969) measured liquid slug frequencies for the carbon dioxide–water system in an 1.9-cm diameter tube. They correlated their data by the following relation (in SI units):

$$\nu_s = 0.0226\left[\frac{u_{LS}}{gD}\left(\frac{19.75}{u_s} + u_s\right)\right]^{1.2} \tag{60}$$

Greskovich and Shrier (1972) used their own data, as well as Hubbard (1965) data and presented the following dimensional correlation for slug frequency in horizontal pipes,

$$\nu_s = 0.0226\left[\lambda\left(\frac{2.02}{D} + \frac{u_s^2}{gD}\right)\right]^{1.2} \tag{61}$$

where λ is the input liquid volumetric quality ($\lambda = u_{LS}/u_s$) and the pipe diameter D is given in meters.

Heywood and Richardson (1979) used the γ-ray absorption method and determined the probability density function and the power spectral densities of the holdup. From these functions they have estimated the average film and slug holdup, the average slug frequency, and the average liquid slug length. They suggested that the slug frequency data may be summarized by the following relation in SI units:

$$\nu_s = 0.0434\left[\lambda\left(\frac{2.02}{D} + \frac{u_s^2}{gD}\right)\right]^{1.02} \tag{62}$$

In all these reports, the slug frequency data exhibit a minimum when plotted versus the mixture velocity u_s and it is a strong function of the liquid flow rate.

As has been mentioned, slug frequency can replace slug length in the auxiliary relation, and the slug length will be an output of the model calculations. We feel, however, that the input of the slug length as an auxiliary variable is preferred to the slug frequency since the slug length is based on a physical model while the slug frequencies are given primarily by experimental correlations.

K. Concluding Remarks

Steady-state slug-flow modeling was presented using a general approach that treats the slug hydrodynamics for vertical, horizontal, and inclined pipes in the same fashion. Critical review of previous work is also presented.

Three methods of solution are presented: (1) the exact method that uses the fully one-dimensional channel-flow solution for the liquid film; (2) the same as (1) with the neglect of pressure drop in the film zone; and

(3) assuming a uniform equilibrium level for the film in the film zone. These three cases differ with regard to the accuracy of the solution and ease of calculations. Case 3 was used primarily for vertical flow and case 2 for horizontal flows. Method 2 however, can be inaccurate for long film zones. Since method 1 is not more difficult to solve than method 2 it is recommended to use method 1 rather than 2.

A special discussion is devoted to the way pressure drop can be calculated. It is shown that there are basically two methods for calculating the pressure drop, namely, (1) using a global momentum balance on a slug unit, and (2) assuming that the pressure drop in the film zone is negligible. In the latter case, the acceleration–pressure drop should be used. It is also shown that when the uniform equilibrium thickness is considered (case 3), the two methods of calculating the pressure drop are not consistent. Based on some numerical examples it seems that when an uniform film thickness is assumed, the calculation for the pressure drop using method (1) is preferred.

Although the present model is probably the most up to date and consistent model for the calculation of the hydrodynamic parameters of steady slug flow and best suited for practical applications, it is still incomplete and some of the approaches used may be regarded as unsatisfactory. Obviously more research has to be performed for the purpose of bringing the theory closer to reality. We would like, at this time, to point out some of the deficiencies that the reader should be aware of.

The most controvertible treatment is the one related to the bubble shape, especially near the bubble nose. We have used different theories to describe the hydrodynamics of the liquid near the bubble nose and the hydrodynamics of the film further upstream, and then we simply superimposed their effect. To predict the drift velocity, two-dimensional potential flow analysis was used, which is different for the horizontal and the vertical case and does not include the inclined case. To the drift velocity we add the propagation velocity (Cu_s) using the notion that the bubble nose follows the highest local velocity of the velocity profile ahead of it. Then the liquid film was analyzed by using the one-dimensional channel-flow equations. Obviously the behavior of the bubble nose and the body of the film should follow a single formulation. Such a formulation would be too complex and probably impractical for pragmatic calculations. There is, however, a genuine need for detailed calculations and experiments in order to improve the understanding of the slug-flow hydrodynamics as well as to provide accurate analysis with which the simple approaches could be compared.

The friction factors used for the liquid slug and the film zones are also of uncertain accuracy. The flow in the liquid slug is not developed, especially in the near-wake region. The use of a fully developed friction factor may be inaccurate. We may also note that the interfacial shear stress is virtually unknown. Accurate data on the interfacial shear may be essential for slugs with very long film zones and high gas velocities.

The theories for determining the liquid holdup in the liquid slug zone R_s, slug length l_s, and slug frequency are also far from being perfect, and considerable work, both experimentally as well as theoretically, should be carried out along these lines.

In spite of the aforementioned deficiencies, of which the reader should be aware, relative simplicity for practical applications is absolutely essential. We do believe that the present model is a reasonable compromise of solid physics and ease of calculations. The scheme presented here is sufficiently flexible to accommodate improvements once more accurate theories or more up-to-date data is available.

III. Severe Slugging

A. Transient Phenomena in Slug Flow

In the previous section steady-state slug flow was considered. In steady slug flow, one is expected to see regular slugs propagating in the pipe. These slugs are of relatively short length (less than $100D$) and separated by regular and evenly spaced elongated bubbles. There are many occasions in which the nature of the slug flow is different than the steady-state flow and has a nonsteady behavior.

An example of transient slugging was given by Taitel *et al.* (1978) when considering unsteady flow of liquid and gas in horizontal pipes. It was shown that one may get temporary slugging of a different nature than that of steady-state slug flow. For example, when one has stratified flow in a pipe and the flow rate of gas is increased slowly, a transition to annular flow will occur. If, however, the increase of the gas flow rate occurs fast, a temporary very long slug will be generated. The occurrence of this phenomenon is easy to explain. In stratified flow the amount of liquid in the pipe is much higher than for the case of annular flow. When suddenly increasing the gas flow rate, there is too much liquid in the pipe for a smooth transition to annular flow. The excess of the liquid is depleted out of the pipe in the form of a very long slug that is being pushed by the gas behind it.

Another example is given by Scott (1987) and Scott *et al.* (1987). In this work, the existence of very large slugs in the Prudhoe Bay 5-km test

[illegible] was explained on the basis of transient pressure fluctuations near the stratified–slug transition boundary. The flow that started as stratified wavy established a high liquid content in the pipe. Due to interfacial instability a slug is generated and starts to move downstream. The high content of the liquid film ahead of the slug is consumed by the advancing slug and causes a fast increase in the slug length. At the pipe entrance stratified flow continue to take place. When a slug exits the pipe, an increase in the pressure drop occurs, which is a cause for a sufficient increase of the gas flow rate to trigger another new slug in the stratified flow zone, and so on. The end result are long slugs that grow rapidly near the entrance zone to sizes that are much longer than the slug size in normal steady-state flow.

The most common unsteady slug flow that is very important for practical application is severe slugging or, as it is also called, terrain-induced slugging. In the general case this type of slugging takes place when a pipeline follows a hilly terrain and the liquid tends to accumulate at the lower valleys blocking the gas passage. The gas upstream is compressed while a long liquid slug grows in the valley. Eventually the pressure upstream increases to the point that it overcomes the gravitational head of the liquid and it pushes the liquid in the valley downstream in the form of a long slug.

A general solution to such a problem is quite complex. The simple case, however, that consists of a single pipeline and a riser, is a common occurrence in offshore oil and gas production and has been analyzed quite successfully. The result of this analysis will be detailed here.

B. Severe Slugging Cycle

Figures 8–11 show the typical behavior of the severe slugging cycle. The first step is the slug formation (Fig. 8). Liquid entering the pipe accumulates at the bottom of the riser, blocks the gas passage and causes the gas in the pipeline to compress. When the liquid height in the riser z reaches the top of the riser $z = h$, the second step of slug movement into the separator starts (Fig. 9). When the gas that is blocked in the pipeline reaches the bottom of the riser the liquid slug is accelerated to high velocity owing to rapid expansion of the gas in the pipeline. This step is termed blowout (Fig. 10). In the last step, Fig. 11, the remaining liquid in the riser falls back to the bottom of the riser and the process of slug formation starts again.

A model for severe slugging was first presented by Schmidt *et al.* (1980). The purpose of such a model is to predict the slug length, slug cycle time, and pressure fluctuations. The following analysis is a simplified version based on the Schmidt *et al.* (1980) analysis.

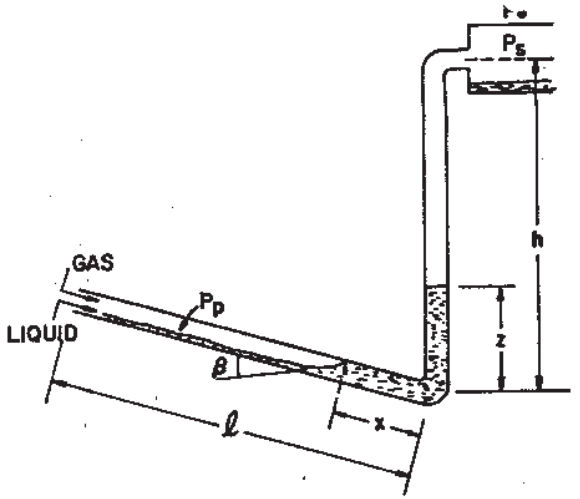

Fig. 8. Slug formation.

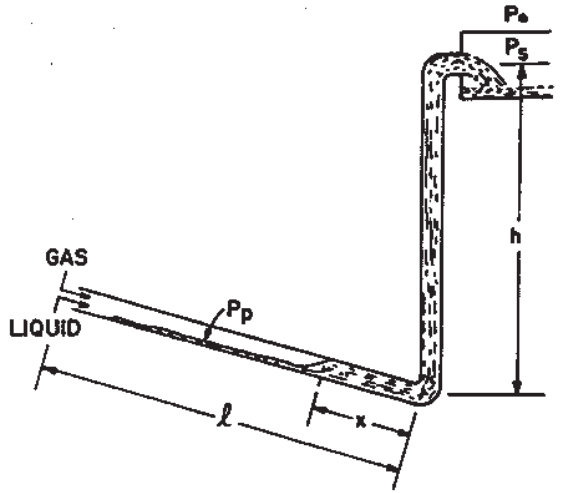

Fig. 9. Slug movement into the separator.

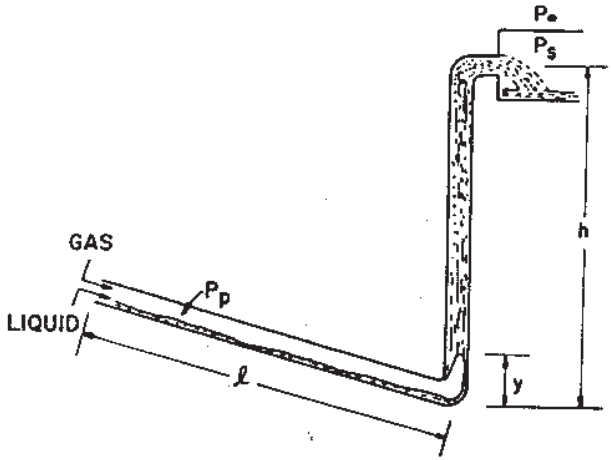

FIG. 10. Blowout.

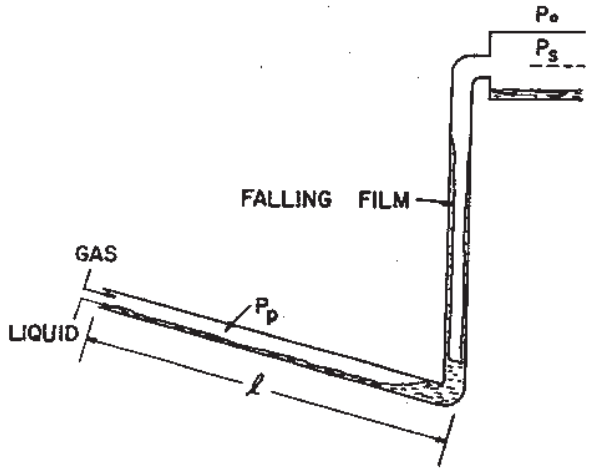

FIG. 11. Liquid fallback.

Since the severe slugging phenomenon is typical of low flow rates of liquid and gas, the pressure is dominated by gravity and the frictional contribution is neglected. The liquid is considered incompressible and the gas is assumed to behave as an ideal gas. Mass inlet flow rates of the liquid and the gas is assumed to be constant. With reference to Fig. 8, $x(t)$ and $z(t)$ can be calculated using the following relations:

Conservation of liquid and gas yields

$$m_L = m_{Li} + \int_0^t A u_{LS} \rho_L \, dt \tag{63}$$

$$m_G = m_{Gi} + \int_0^t A u_{GS0} \rho_{G0} \, dt \tag{64}$$

where m_{Li} is the initial value of the liquid in the system and m_{Gi} is the initial value of the gas in the pipeline. The determination of these initial values will be discussed later.

The mass of liquid and gas can be written in terms of the values of x and z as

$$m_L = \rho_L A(x + z) + (1 - \alpha)\rho_L A(l - x) \tag{65}$$

$$m_G = \rho_G V_G = \frac{P_p}{RT} V_G = \frac{P_s + \rho_L g(z - x \sin \beta)}{RT} [(l - x)\alpha + L]A \tag{66}$$

(LA) is an additional gas volume that may exist between the gas inlet valve and the liquid inlet. Usually L is zero for most practical applications. It is, however, convenient to use $L > 0$ in experimental facilities (Taitel *et al.*, 1989) to simulate longer pipeline performance when the actual pipeline length l is short. Note that m_{Li} and m_{Gi} are given by Eqs. (65) and (66) for $x = x_i$ and $z = z_i$. Equations (63) and (64) are sufficient to solve for x, z, and P_p as a function of time provided the initial values of x and z (x_i and z_i) and the void fraction in the pipeline α are known. The determination of these initial values will be discussed later.

Substituting m_G and m_{Gi} from Eq. (66) in Eq. (64) yields for the gas,

$$\left[\frac{P_s}{\rho_L g} + (z - x \sin \beta)\right][(l - x)\alpha + L] = \left[\frac{P_s}{\rho_L g} + (z_i - x_i \sin \beta)\right][(l - x_i)\alpha + L] + \frac{RT}{\rho_L g} \int_0^t u_{GS0} \rho_{G0} \, dt \tag{67}$$

Substituting m_L and m_{Li} from Eq. (65) into Eq. (63) yields, for the liquid,

$$z = z_i - \alpha(x - x_i) + \int_0^t u_{LS} \, dt \tag{68}$$

Equations (67) and (68) can be solved now for $x(t)$ and $z(t)$, which correspond to the slug formation step (Fig. 8). Once the slug reaches the top of the riser ($z = h$) the process is continued as shown in step 2 (Fig. 9). Thus, after $z = h$ the solution for $x(t)$ is obtained directly from Eq. (67) with $z = h$.

The initial values of x_i and z_i depend on the amount of liquid that stays in the riser at the end of the blowout process (Figs. 10 and 11). The blowout process is usually a highly chaotic phenomenon and the prediction of the liquid fallback is difficult. Schmidt *et al.* (1980) used an experimental correlation to estimate the amount of fallback. Taitel (1986) assumed that the blowout process is in the form of a single fast-moving Taylor bubble. In this case the liquid film left in the riser can be calculated on the basis of a slug-flow model. The result of such calculations showed that the void fraction of such a Taylor bubble α' is around 10%. Assuming that at the beginning of the fallback the pressure in the pipeline is P_s, that the falling liquid blocks the air passage, and that the fallback is very fast, then one can calculate x_i, z_i, and P_p using the following relations: Hydrostatic pressure:

$$P_p = P_s + \rho_L g(z_i - x_i \sin\beta) \tag{69}$$

Liquid mass balance requires

$$\alpha x_i + z_i = (1 - \alpha')h \tag{70}$$

while the compression of the gas in the pipeline follows the relation

$$P_p = P_s \frac{l\alpha + L}{(l - x_i)\alpha + L} \tag{71}$$

The calculation of the void fraction α in the pipeline can be calculated using a steady-state stratified flow in an inclined pipeline (Taitel and Dukler, 1976). Furthermore, since the flow of the liquid and gas is usually low (this is the *a priori* condition for severe slugging), the void fraction can be calculated as in an open channel flow. In this case a momentum balance of shear stress and gravity on the liquid phase yields

$$\tau_L S_L = \rho_L g A_L \sin\beta \tag{72}$$

where

$$\tau_L = f_L(\rho_L u_L^2/2) \tag{73}$$

The friction factor f_L can be calculated from the Moody diagram with the appropriate hydraulic diameter. For smooth pipes, for example, the friction factor can be calculated by

$$f_L = C_L(4A_L u_L/S_L \nu_L)^{-n} \tag{74}$$

where $C_L = 0.046$ and $n = 0.2$ for turbulent flow, and $C_L = 16$ and $n = 1$ for laminar flow. The cross-sectional area A_L and the wetting periphery S_L are given in terms of the equilibrium liquid level h_L [see Eqs. (39) and (41)]. Equation (73) can now be solved for the equilibrium level h_L. Once h_L is given the void fraction α can be calculated by

$$\alpha = 1 - (A_L/A) \tag{75}$$

The theory presented here provides sufficient means to calculate some of the major parameters of severe slugging such as the fluctuation of the pressure in the line $P_p(t)$, the length of penetration of the liquid into the pipeline $x(t)$, the slug length that enters the separator, and the cycle time of the process.

C. Boe's Criterion for Severe Slugging

The severe slugging pattern is typical of relatively low liquid and gas flow rates. It requires that the flow pattern in the pipeline be stratified. Thus, one condition for the existence of severe slugging is that the flow pattern in the inclined pipeline will be in the stratified flow pattern. For the determination of this condition, one needs to use flow pattern maps or any flow pattern prediction methods (Taitel and Dukler, 1976; Barnea, 1987).

In addition to this condition, the existence of a severe slugging cycle requires that the liquid will penetrate into the pipeline, namely, $x > 0$ (Boe, 1981). This requirement is usually satisfied for a relatively low gas flow rate. Referring to Fig. 8, the condition for x to stay at zero is when the increase of the pressure owing to the addition of liquid into the riser is balanced by the increase in the pipeline pressure due to the addition of gas. The increase of pressure owing to the addition of liquid is

$$dP_p/dt = \rho_L g(dz/dt) = \rho_L g u_{LS} \tag{76}$$

The increase of pressure owing to the addition of gas is

$$\frac{dP_p}{dt} = \frac{\dot{m}_G}{V_G} RT = \frac{u_{GS0}\rho_{G0}}{l\alpha + L} RT = \frac{P_p u_{GS}}{l\alpha + L} \tag{77}$$

Equating the right-hand sides of Eqs. (76) and (77) yield the transition boundary proposed by Boe between the severe slugging pattern and a steady flow in the riser (usually bubbly or slug flow):

$$u_{LS} = \frac{P_p}{\rho_L g(l\alpha + L)} u_{GS} \quad \text{or} \quad u_{LS} = \frac{\rho_{G0} RT}{\rho_L g(l\alpha + L)} u_{GS0} \tag{78}$$

Equation (78) can also be derived on the basis of our previous development. Setting x and x_i to zero in Eq. (67) leads to the same condition as Eq. (78).

Equation (78) is shown by the boundary A on Fig. 12 for a specific example reported by Taitel *et al.* (1989). Note that at low liquid flow rates,

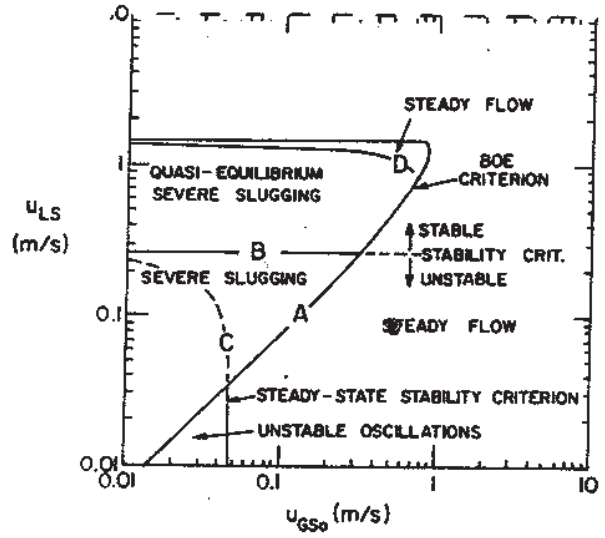

FIG. 12. Occurrence of severe slugging in an air–water system at 25°C: $P_s = 0.1$ MPa, $D = 2.54$ cm, $l = 9.1$ m, $L = 5.1$ m, $h = 3$ m, $\beta = -5°$ (after Taitel *et al.*, 1989).

u_{LS} is a monotonic linear function of the gas inlet flow rate u_{GS0}. For high liquid flow rates α approaches 0 and the curve is bent to the left. Note, however, that α here is calculated while neglecting the gas shear [Eq. (72)]. Thus this upper limit is beyond the applicability of the present calculations.

Boe claimed that outside the region bounded by A the flow will be of steady-state nature while inside severe slugging will prevail. This claim, however, will be shown to be not quite accurate. In fact the Boe criterion may be violated and one may get steady-state flow within the region designated by Boe as severe slugging and vice versa, one can get severe slugging in the region designated by the Boe criterion as steady-state flow. The occurrence of such anomalies will be discussed next.

D. Stability Criterion

The stability criterion addresses itself to the blowout step of the severe cycle process. As discussed earlier the blowout process (Fig. 10) was assumed to take place in the form of a spontaneous expansion of the gas in the pipeline. Indeed this is usually the case. The criterion for determining the condition under which a vigorous blowout will occur versus a quasi-equilibrium penetration is termed here the stability criterion (Taitel, 1986).

Assume that the cycle of severe slugging reaches the point at which the liquid slug tail has just entered the riser. Assume a small disturbance y that carries the liquid somewhat higher (see Fig. 10) and that the disturbance is fast enough so that the slow flow rates of liquid and gas are ignored while y changes.

The net force (per unit area) acting on the liquid in the riser is

$$\Delta F = \left[(P_s + \rho_L g h)\frac{\alpha l + L}{\alpha l + L + \alpha' y}\right] - [P_s + \rho_L g(h - y)] \tag{79}$$

The first term on the right-hand side is the pipeline pressure driving force. The pressure varies with y as a result of the expansion of the gas in the pipeline. The second term corresponds to the back pressure force applied by the separator pressure and the liquid column of density ρ_L and height $(h - y)$. Note that for $y = 0$ the system is in equilibrium and $\Delta F = 0$. In Eq. (79) α' is the gas holdup in the gas cap penetrating the liquid column; α' can be estimated on the basis of a slug-flow model. Also, the gas is assumed to expand isothermally following the ideal gas law.

The liquid column will be blown out of the pipe if ΔF increases with y. Thus, the condition for stability is

$$\partial(\Delta F)/\partial y < 0 \qquad \text{at} \quad y = 0 \tag{80}$$

This leads to the criterion for stability

$$\frac{P_s}{P_0} > \frac{[(\alpha l + L)/\alpha'] - h}{P_0/\rho_L g} \tag{81}$$

where P_0 is the atmospheric, or reference, pressure.

Equation (81) is shown in Fig. 12 by boundary B, which divides the region bounded by the Boe criterion into two subregions. The region below line B is unstable and the blowout process is vigorous. The region above B is characterized by a quasi-equilibrium penetration of the gas into the liquid. Taitel *et al.* (1989) showed that this penetration can end up either with steady flow in the riser or it can develop into a cyclic operation. The latter is termed quasi-equilibrium severe slugging (to be discussed in the next section).

The stability criterion [Eq. (81)] was applied within the region bounded by curve A (Boe criterion). However, this criterion can also be used outside this region where a steady-state flow is assumed to take place (Taitel, 1986). Indeed, it can be shown that an unstable subregion exists outside Boe's region. In this region a severe slugging process will take place as follows: gas in the pipeline will spontaneously expand into the riser and a blowout will occur, followed by liquid fallback. Thereafter, gas will

continue to penetrate into the riser and bubble through it while the liquid (mixture) level in the riser, z, rises towards the top of the riser. At the time the liquid level reaches the top of the riser, a steady state is expected to ensue. However, because of the inherent lack of stability, blowout will reoccur. This gives rise to a cyclic severe slugging process except that the slugs produced into the separator are aerated and shorter than the riser length, unlike the classic severe slugging.

The criterion for the existence of severe slugging under such conditions is obtained using Eq. (81) in which ρ_L is replaced by $\rho_L\bar{\Phi}$, where $\bar{\Phi}$ is the average liquid holdup in the riser under steady-state conditions (the gas density can be ignored).

The value of $\bar{\Phi}$ is obtained by using Eq. (9). Assuming unaerated liquid slugs in the riser, the value of average liquid holdup under steady-state condition is

$$1-\bar{\Phi}=u_{GS}/[C(u_{GS}+u_{LS})+u_d] \tag{82}$$

Note that Eq. (82) is also valid for bubbly flow in the riser in which case C and u_d are replaced by B and u_0.

The gas superficial velocity in the riser, adjusting for the average pressure in the riser, is given by

$$u_{GS}=u_{GS0}\frac{P_0}{P_s+\rho_L\bar{\Phi}gh/2} \tag{83}$$

Equations (82) and (83) yield the liquid holdup $\bar{\Phi}$ in steady state. The stability of this steady state can be evaluated by Eq. (81) (using $\bar{\Phi}\,\rho_L$). The line of marginal stability is shown in Fig. 12 for the case of slug flow by line C. As can be seen, there is a definite region in which one can obtain unstable steady-state flow outside Boe's region. As a result the flow will be cyclic similar to the severe slugging cycle. We term this cyclic behavior as unstable oscillations.

E. Quasi-Equilibrium Severe Slugging

The region above line B in Fig. 12, although found to be stable according to Eq. (81), may behave in a cyclic fashion termed quasi-equilibrium steady state. In this case it is possible to calculate and predict the behavior of the riser during this process, enabling also to predict whether the system will end up in a steady state or a cyclic operation.

The analysis begins at the point when the riser is full of liquid and gas is just entering the bottom of the riser under equilibrium conditions. We assume that the condition is stable so that no blowout occurs as a result of the penetration of the gas into the riser. Nevertheless, when gas enters the riser the hydrostatic pressure at the bottom of the riser decreases. This causes an expansion of the gas in the pipeline. As a result the mass flow rate of gas into the riser $\dot{m}_G$ increases. Assuming ideal gas behavior, the instantaneous mass flow rate into the riser can be calculated by

$$\dot{m}_G=\dot{m}_{Gin}-\frac{(\alpha l+L)A}{RT}\frac{dP_p}{dt} \tag{84}$$

The pressure in the pipeline (and at the bottom of the riser) is the hydrostatic pressure exerted by the weight of the liquid column in the riser (the gas weight is neglected). Designating the local liquid holdup in the pipe as Φ, one obtains that

$$P_p=P_s+\int_0^h \Phi\rho_L g\,dy \tag{85}$$

The gas that penetrates the bottom of the riser is in the form of either small bubbles or larger Taylor bubbles. In either case it is assumed that the gas velocity equals the translational velocity, which is given in the form of Eq. (37).

In Eq. (37) u_s is the mixture velocity in the liquid slug. Note that this mixture velocity is equal to the total superficial velocity, $u_S(u_S=u_{LS}+u_{GS})$. In order to simplify the problem a constant superficial velocity u_S is assumed. For this purpose we calculate the average gas density as

$$\bar{\rho}_G=\int_0^h(1-\Phi)\frac{P}{RT}dy\Big/\int_0^h(1-\Phi)\,dy \tag{86}$$

As can be seen in Eq. (86) the average gas density is calculated based on the local pressure in the riser weighted by the local gas void fraction $(1-\Phi)$. The local pressure is given by

$$P(y)=P_s+\int_y^h \Phi\rho_L g\,dy \tag{87}$$

Using Eq. (86), the superficial gas velocity in the riser is

$$u_{GS}=\frac{\dot{m}_G}{\bar{\rho}_G A} \tag{88}$$

Note that although u_S is assumed to be constant along the pipe, it is a function of time.

The liquid holdup at the bottom of the riser is given by

$$\Phi_b=1-(u_{GS}/u_t) \tag{89}$$

The local liquid holdup in the riser is determined by simple propagation of the liquid holdup at the bottom of the riser with a velocity u_t. Thus, the

local pressure and liquid holdup

$$\Phi(y) = \Phi_b \qquad \text{on} \quad y = \int_0^t u_t\, dt \tag{90}$$

This mathematical formulation allows one to calculate the variation of the pipeline pressure, gas mass flow rate into the riser as a function of time, and the local instantaneous liquid holdup in the riser $\Phi(y,t)$. Although the formulation is somewhat complex, it is very simple to program using an explicit Lagrangian numerical scheme described next.

At time $t=0$ the riser is full of liquid, $\Phi = 1$ and $\dot{m}_G = \dot{m}_{Gin}$. The average density of the gas at this time is the inlet density. The gas superficial velocity is given by Eq. (88) and the translational velocity is calculated by Eq. (37). The riser is subdivided into small segments of length Δh and the time step Δt is calculated using $\Delta t = \Delta h/u_t$.

After time Δt, Φ_1 (at the bottom of the riser, $=\Phi_b$) is given by Eq. (89); the new pressure is given by Eq. (85); the new average gas density in the riser is given by Eq. (86); and the new gas mass flow rate into the riser is given by Eq. (84). Note that dP/dt in Eq. (84) is approximated numerically by the difference between the new and old pressure divided by Δt. Once the new $\dot{m}_G$ is known, the new gas superficial velocity u_{GS} is calculated from Eq. (88) along with the new translational velocity u_t from Eq. (37) and the new time step Δt ($\Delta t = \Delta h/u_t$).

At the next time step, Φ_{j+1} is set equal to Φ_j and this takes care of the propagation of the bubbles in the riser; Φ_1 is calculated as before.

This analysis can be used provided the penetration of the gas into the riser $\dot{m}_G$ is always positive (which leads finally to a steady-state flow). Boundary D on Fig. 12 is the curve above which the flow will indeed reach a steady state. As seen, a steady state can take place within the Boe region. In the particular example of Fig. 12 boundary D is very close to the upper Boe region. Obviously the region of steady flow within the Boe region can be larger for different operating conditions. Below boundary D $\dot{m}_G$ is not always positive, resulting in penetration of the liquid into the pipeline. Let $x(t)$ be the distance of the liquid interface penetrating into the pipeline. Under hydrostatic equilibrium the pipeline pressure at any time is

$$P_p = \rho_L g(\bar{\Phi} h - x \sin\beta) + P_s \tag{91}$$

where $\bar{\Phi}$ is the average liquid holdup in the riser. A mass balance on the gas in the pipeline requires that [see Eq. (67)]

$$\left[\frac{P_s}{\rho_L g} + (\bar{\Phi} h - x\sin\beta)\right][(l-x)\alpha + L] = \left[\frac{P_s}{\rho_L g} + \bar{\Phi}_i h\right](l\alpha + L) + \frac{RT}{A\rho_L g}\int_{t_i}^{t} \dot{m}_{Gin}\, dt \tag{92}$$

where i relates to the time when $m_G = 0$ and penetration of liquid into the pipe starts.

Equation (92) can be solved for x as a function of time. For this purpose the average liquid holdup $\bar{\Phi}$ should be known as a function of time. The variation of $\bar{\Phi}$ with time can be calculated as before on the basis of the translational velocity u_t from Eq. (37). The calculation of the mixture velocity u_S is then calculated on the basis of the liquid mass balance to yield

$$u_S = u_{LS} - \alpha\,(dx/dt) \tag{93}$$

At time t_i, $x = 0$ and $u_S = u_{LS}$ ($\dot{m}_G = u_{GS} = 0$). For time step Δt, we then calculate the new Φ distribution in the riser and $\bar{\Phi}$, the new x, the new u_s (approximately dx/dt numerically), the new u_t, and the new step Δt. As in the case of severe slugging, x increases to a maximum and than recedes back to zero. When $x = 0$ the cyclic process is repeated.

This calculation is valid provided no fallback occurs. A condition of fallback is defined when the top of the riser becomes clear of liquid (or liquid mixture) and a visible liquid interface is propagating towards the top of the riser. The condition of fallback is related to the net liquid velocity at the top of the riser. Once the liquid velocity at the top of the riser is less than zero no liquid exits the riser, resulting in fallback of the liquid in the riser. Thus, the point at which fallback occurs is when u_L is negative, where u_L at the top is given by (simple mass balance)

$$u_L = \frac{u_S - u_t(1-\Phi_{top})}{\Phi_{top}} \tag{94}$$

Once this situation occurs we calculate the liquid height in the riser by $z = z_i = \bar{\Phi} h$ and the calculation proceeds in the exact manner described before for the classic severe slugging. In this calculation $x(t)$ as well as $z(t)$ are calculated on the basis of two equations, Eq. (95), which is a mass balance on the gas [similar to Eqs. (92) and (67)],

$$\left[\frac{P_s}{\rho_L g} + (z - x\sin\beta)\right][(l-x)\alpha + L] = \left[\frac{P_s}{\rho_L g} + z_i h\right][(l-x_i)\alpha + L] + \frac{RT}{A\rho_L g}\int_{t_i}^{t} \dot{m}_{Gin}\, dt \tag{95}$$

and Eq. (96), which is a mass balance on the liquid

$$z = z_i - \alpha(x - x_i) + \int_{t_i} u_{LS}\, dt \tag{96}$$

Equations (93) and (96) are used to calculate $x(t)$ and $z(t)$. Once the slug reaches the top of the riser, then $z = h$, and $x(t)$ is calculated by Eq. (95) only. The values of x_i and z_i are the values of x and z at the time of fallback, namely when u_L becomes negative. As in the previous case, once x recedes to zero, the gas penetrates the riser and the cycle is repeated.

F. Summary and Conclusions

The severe slugging that consists of one riser and one pipeline is perhaps one of the simplest examples of slug flow under nonsteady conditions. As is evident, even this simple case is not at all trivial and presents quite a number of possible operating conditions. A more detailed discussion and experimental verification of the present theory is given by Taitel *et al.* (1989) and Vierkandt (1988). A summary of the results is presented using an example of a typical flow map as shown in Fig. 12. This map contains four boundaries: A—the Boe criterion, B—the stability criterion, C—the steady-state stability criterion, and D—the transition to steady flow inside the Boe criterion.

The Boe criterion [Eq. (78)] differentiates quite well between steady and cyclic operations with two exceptions. At high liquid flow rates, a steady flow can also exist within the severe slugging region predicted by the Boe criterion (above boundary D). Also there is a region outside the Boe criterion that is in an unsteady state and leads to unsteady oscillations (between boundaries C and A).

The stability criterion [Eq. (81)] is applied to the cases of severe slugging (inside the Boe region) where the riser contains only liquid (B), and to the case of steady flow of liquid and gas in the riser (C) (outside the Boe region). The former is an approximate boundary dividing between classical and quasi-equilibrium severe slugging cyclic operations. The latter indicates when steady flow outside the Boe criterion is not possible and one obtains unsteady oscillations.

Unlike boundaries A, B, and C, which are given by simple equations, the condition for boundary D is a more complex one and is obtained during a numerical solution of the quasi-equilibrium case as a dividing line between cases where the gas flow rate into the riser is always positive ($\dot{m}_G > 0$) and the cases where $\dot{m}_G$ reaches zero in the cyclic process. Note that in Fig. 12, curve D is very close to the upper boundary of Boe criterion. This is not always the case and, in fact, this boundary can be substantially lower and also higher than the Boe criterion (in which case it is not applicable), depending primarily on the length of the pipeline (l and L) (Taitel *et al.*, 1989).

Nomenclature

A	pipe cross-sectional area
b	interface width in the pipe
B	constant in Eq. (38)
C	constant in Eq. (37) and in the friction factor correlation
D	pipe diameter
d	bubble diameter
f	friction factor
F	force
g	acceleration of gravity
h	liquid level and riser height
l	pipe length
L	additional equivalent gas pipeline length
m	mass
n	constant in the friction factor correlation
r	pipe radius
P	pressure
q	local absolute velocity
R	liquid holdup, also ideal gas constant
Re	Reynolds number
S	wetted periphery
t	time
T	absolute temperature
u	velocity in the axial direction
U	free-steam velocity
v	relative velocity, usually relative to the translational velocity
V	volume
x	coordinate in the downstream direction, also distance of liquid penetration into the pipeline
X	mass flow rate relative to the translational velocity
y	coordinate in the perpendicular to the pipe axis direction, also vertical coordinate in the riser
W	mass flow rate
z	coordinate in the upstream direction, also liquid height in the riser
α	void fraction
β	angle of inclination
γ	polar angle that defines the interface
δ	film thickness
ε	roughness
θ	polar coordinate
λ	liquid volumetric quality, u_{LS}/u_S
μ	viscosity
ν	kinematic viscosity, also frequency
ρ	density
σ	surface tension
Σ	surface tension parameter, $\sigma/[(\rho_L - \rho_G)gr^2]$
τ	shear stress
Φ	liquid holdup in the riser

Subscripts and Superscripts

acc	accelaration
b	bubble
c	critical
d	drift
E	equilibrium
f	film
fe	film at $z = l_f$
fi	film at $z = 0$
G	gas
h	hydraulic, also horizontal
i	interface, also initial
in	inlet
j	discretization index in the riser
L	liquid
mix	related to mixing
0	free rise, also at standard atmospheric conditions
p	pipeline
s	slug, also separator
S	superficial
t	translational
top	top of the riser
u	slug unit
v	vertical
∞	for unbounded liquid

Special Symbols

$\bullet$	rate
$\bar{\ }$	average

Akagawa, K., and Sakaguchi, T. Fluctuation of void ratio in two-phase flow (2nd report, analysis of flow configuration considering the existence of small bubbles in liquid slugs). *Bull. JSME* **9**, 104–110 (1966).

Andritsos, N., and Hanratty, T. J. Interfacial instabilities for horizontal gas–liquid flows in pipelines. *Int. J. Multiphase Flow* **13**, 583–603 (1987).

Barnea, D. A unified model for predicting flow pattern transitions in the whole range of pipe inclination. *Int. J. Multiphase Flow* **13**, 1–12 (1987).

Barnea, D. Effect of bubble shape on pressure drop calculations in vertical slug flow. *Int. J. Multiphase Flow* in press (1989).

Barnea, D., and Brauner, N. Hold-up of the liquid slug in two phase intermittent flow. *Int. J. Multiphase Flow* **11**, 43–49 (1985).

Barnea, D., and Shemer, L. Void fraction measurements in vertical slug flow: Applications to slug characteristics and transition. *Int. J. Multiphase Flow* **15**, 495–504 (1989).

Barnea, D., Shoham, O., and Taitel, Y. Flow pattern characterization for two phase flow by electrical conductance probe. *Int. J. Multiphase Flow* **6**, 387–397 (1980).

Barnea, D., Shoham, O., Taitel, Y., and Dukler, A. E. Gas–liquid flow in inclined tubes: Flow pattern transitions for upward flow. *Chem. Eng. Sci.* **40**, 131–136 (1985).

Barr, G. The air-bubble viscometer. *Philos. Mag.* **1**, 395–405 (1926).

Bendiksen, K. H. An experimental investigation of the motion of long bubbles in inclined tubes. *Int. J. Multiphase Flow* **10**, 467–483 (1984).

Bendiksen, K. H. On the motion of long bubbles in vertical tubes. *Int. J. Multiphase Flow* **11**, 797–812 (1985).

Benjamin, T. B. Gravity currents and related phenomena. *J. Fluid Mech.* **31**, Part 2, 209–248 (1968).

Boe, A. Severe slugging characteristics. *Sel. Top. Two-Phase Flow, NTH, Trondheim, Norw.* (1981).

Bonnecaze, R. H., Eriskine, W., Jr., and Greskovich, E. J. Holdup and pressure drop for two-phase slug flow in inclined pipelines. *AIChE J.* **17**, 1109–1113 (1971).

Brauner, N., and Barnea, D. Slug/churn transition in upward gas–liquid flow. *Chem. Eng. Sci.* **41**, 159–163 (1986).

Brodkey, R. S. "The Phenomena of Fluid Motions." Addison-Wesley, Reading, Massachusetts, (1967).

Cohen, S. L., and Hanratty, T. J. Effects of waves at a gas–liquid interface on a turbulent air flow. *J. Fluid Mech.* **31**, 467–469 (1968).

Collins, R., De Moraes, F. F., Davidsom, J. F., and Harrison, D. The motion of a large gas bubble rising through liquid flowing in a tube. *J. Fluid Mech.* **89**, Part 3, 497–514 (1978).

Davies, R. M., and Sir Taylor, G. (F. R. S). The mechanics of large bubbles rising through extended liquids and through liquids in tubes. *Proc. R. Soc. London, Ser. A* **200**, 375–390 (1949).

Dukler, A. E., and Hubbard, M. G. A model for gas–liquid slug flow in horizontal and near horizontal tubes. *Ind. Eng. Chem. Fundam.* **14**, 337–347 (1975).

Dukler, A. E., Moalem-Maron, D., and Brauner, N. A physical model for predicting the minimum stable slug length. *Chem. Eng. Sci.* **40**, 1379–1385 (1985).

Dumitrescu, D. T. Stromung an einer luftblase im senkrechten rohr. *Z. Angew. Math. Mech.* **23**, 139–149 (1943).

Fernandes, R. C. Experimental and theoretical studies of isothermal upward gas–liquid flows in vertical tubes. Ph. D. Thesis, University of Houston, Houston, Texas, (1981).

Fernandes, R. C., Semiat, R., and Dukler, A. E. Hydrodynamic model for gas–liquid slug flow in vertical tubes. *AIChE J.* **29**, 981–989 (1983).

Goldsmith, H. L., and Mason, S. G. The movement of single large bubbles in closed vertical tubes. *J. Fluid Mech.* **14**, 42–58 (1962).

Govier, G. W., and Aziz, K. "The Flow of Complex Mixtures in Pipes." Van-Nostrand-Reinhold, Princeton, New Jersey, 1972.

Gregory, G. A., and Scott, D. S. Correlation of Liquid slug velocity and frequency in horizontal cocurrent gas–liquid slug flow. *AIChE J.* **15**, 933–935 (1969).

Gregory, G. A., Nicholson, M. K., and Aziz, K. Correlation of the liquid volume fraction in the slug for horizontal gas–liquid slug flow. *Int. J. Multiphase Flow* **4**, 33–39 (1978).

Greskovich, E. J., and Shrier, A. L. Pressure drop and holdup in horizontal slug flow. *AIChE J.* **17**, 1214–1219 (1971).

Greskovich, E. J., and Shrier, A. L. Slug frequency in horizontal gas–liquid slug flow. *Ind. Eng. Chem. Process Des. Dev.* **11**, 317–318 (1972).

Hall, N. A. "Thermodynamics of Fluid Flow." Longmans, Green, New York, (1957).

Harmathy, T. Z. Velocity of large drops and bubbles in media of infinite of restricted extent. *AIChE J.* **6**, 281–288 (1960).

Hasan, A. R., and Kabir, C. S. Predicting multiphase flow behavior in a deviated well. *61st Annu. Tech. Conf. New Orleans, La.* SPE 15449 (1986).

Henderson, F. M. "Open Channel Flow." Macmillan, New York, (1966).

Heywood, N. I., and Richardsom, J. F. Slug flow of air–water mixtures in a horizontal pipe: determination of liquid holdup by gama-ray absorption. *Chem. Eng. Sci.* **34**, 17–30 (1979).

Hubbard, M. G. An analysis of horizontal gas–liquid slug flow. Ph. D. Thesis, University of Houston, Houston, Texas, 1965.

Kouba, G. E. Horizontal slug flow modeling and metering. Ph. D. Thesis, University of Tulsa, Tulsa, Oklahoma, 1986.

Levich, V. G. "Physicochemical Hydrodynamics." Prentice-Hall, Englewood Cliffs, New Jersey, 1962.

Mandhane, J. M., Gregory, G. A., and Aziz, K. A flow pattern map for gas–liquid flow in horizontal pipes. *Int. J. Multiphase Flow* **1**, 537–553 (1974).

Marrucci, G. An interpretation of slip in horizontal gas–liquid slug flow. *Chem. Eng. Sci.* **21**, 718–719 (1966).

Moissis, R. The transition from slug to homogeneous two-phase flows. *J. Heat Transfer* **85**, 366–370 (1963).

Moissis, R., and Griffith, P. Entrance effects in a two-phase slug flow. *J. Heat Transfer* **84**, 29–39 (1962).

Nicholson, M. K., Aziz, K., and Gregory, G. A. Intermittent two phase flow in horizontal pipes: predictive models. *Can. J. Chem. Eng.* **56**, 653–663 (1978).

Nicklin, D. J. Two-phase bubble flow. *Chem. Eng. Sci.* **17**, 693–702 (1962).

Nicklin, D. J., Wilkes, J. O., and Davidson, J. F. Two-phase flow in vertical tubes. *Trans. Inst. Chem. Eng.* **40**, 61–68 (1962).

Orell, A., and Rembrand, R. A model for gas–liquid slug flow in a vertical tube. *Ind. Eng. Chem. Fundam.* **25**, 196–206 (1986).

Schmidt, Z. Experimental study of two-phase slug flow in a pipeline-riser pipe system. Ph. D. Thesis, University of Tulsa, Tulsa, Oklahoma, 1977.

Schmidt, Z., Brill, J. P., and Beggs, H. D. Experimental study of severe slugging in a two-phase flow pipeline-riser pipe system. *Soc. Pet. Eng. J.* **20**, 407–414. (1980).

Scott, S. L. Modeling slug growth in pipelines. Ph. D. Thesis, University of Tulsa, Tulsa, Oklahoma, 1987.

Scott, S. L., Shoham, O., and Brill, J. P. Modelling slug growth in large diameter pipes. *Proc. Int. Conf. Multi-Phase Flow, 3rd, The Hague* pp. 55–63 (1987).
Shemer, L., and Barnea, D. Visualization of the instantaneous velocity profiles in gas–liquid slug flow. *Physicochem. Hydrodyn.* **8**, 243–253 (1987).
Shoham, O., and Taitel, Y. Stratified turbulent–turbulent gas liquid flow in horizontal and inclined pipes. *AIChE J.* **30**, 377–385 (1984).
Singh, G., and Griffith, P. Determination of the pressure drop optimum pipe size for a two-phase slug flow in an inclined pipe. *J. Eng. Ind.* **92**, 717–726 (1970).
Stanislav, J. F., Kokal, S., and Nicholson, M. K. Intermittent gas–liquid flow in upward inclined pipes. *Int. J. Multiphase Flow* **12**, 325–335 (1986).
Sylvester, N. D. A mechanistic model for two phase vertical slug flow in pipes. *J. Energy Resour. Technol.* **109**, 206–213 (1987).
Taitel, Y. Stability of severe slugging. *Int. J. Multiphase Flow* **2**, 203–217 (1986).
Taitel, Y., and Barnea, D. A consistent approach for calculating pressure drop in inclined slug flow. *Chem. Eng. Sci.* submitted (1989).
Taitel, Y., and Dukler, A. E. A model for prediction flow regime transitions in horizontal and near horizontal gas–liquid flow. *AIChE J.* **22**, 47–55 (1976).
Taitel, Y., and Dukler, A. E. A model for slug frequency during gas liquid flow in horizontal and near horizontal pipes. *Int. J. Multiphase Flow* **3**, 585–596 (1977).
Taitel, Y., Lee, N., and Dukler, A. E. Transient gas–liquid flow in horizontal pipes—modeling flow pattern transitions. *AIChE. J.* **24**, 920–935 (1978).
Taitel, Y., Barnea, D., and Dukler, A. E. Modelling flow pattern transitions for steady upward gas–liquid flow in vertical tubes. *AIChE J.* **26**, 345–354 (1980).
Taitel, Y., Vierkandt, S., Shoham, O., and Brill, J. P. Severe slugging in a pipeline-riser system, experiments and modeling. *Int. J. Multiphase Flow* in press (1989).
Taylor, G. I. Deposition of a viscous fluid on the wall of a tube. *J. Fluid Mech.* **10**, 161–165 (1961).
Vierkandt, S. Severe slugging in a pipeline-riser system, experiments and modeling. M. S. Thesis, University of Tulsa, Tulsa, Oklahoma, 1988.
Wallis, G. B. "One Dimensional Two-Phase Flow." McGraw-Hill, New York, 1969.
Wallis, G. B., Richter, H. J., and Bharathan, D. "Air–Water Countercurrent Annular Flow in Vertical Tubes." Rep. EPRI NP-786. Electr. Power Res. Inst. Palo Alto, Calif., 1978.
Wallis, G. B., Richter, H. J., and Bharathan, D. "Air–Water Countercurrent Annular Flow in Vertical Tubes." Rep. EPRI NP-1165. Electr. Power Res. Inst. Palo Alto, Calif., 1979.
Weber, M. E. Drift in intermittent two-phase flow in horizontal pipes. *Can. J. Chem. Eng.* **59**, 398–399 (1981).
Weisman, J., Duncan, D., Gibson, J., and Crawford, T. Effect of fluid properties and pipe diameter on two-phase flow pattern in horizontal lines. *Int. J. Multiphase Flow* **5**, 437–460 (1979).
Zuber, N., and Findlay, J. A. Average volumetric concentration in two-phase flow systems. *J. Heat Transfer* **87**, 453–468 (1965).
Zuber, N., and Hench, J. "Steady State and Transient Void Fraction of Bubbling Systems and Their Operating Limit. Part I: Steady State Operation," Rep. 62GL100. Gen. Electr., Schenectady, N. Y., 1962.
Zukoski, E. E. Influence of viscosity, surface tension, and inclination angle on motion of long bubbles in closed tubes. *J. Fluid Mech.* **25**, 821–837 (1966).

Unified Regenerator Theory and Reexamination of the Unidirectional Regenerator Performance

BRANISLAV S. BACLIC

Technicki Fakultet Mihajlo Pupin, University of Novi Sad, 23000 Zrenjanin, Yugoslavia

PETER J. HEGGS

Department of Chemical Engineering, University of Bradford, Bradford, England

I Introduction

The simplest mathematical representation of fixed-bed cyclic thermal regenerators has remained virtually static since the initial publications of Nusselt [1] and Hausen [2], and likewise, the rotary-matrix exchanger has also stayed in the same state since the original work of Coppage and London [3]. In both systems, the sole mechanism of heat transfer between the flowing gases and the regenerator matrix is assumed to be forced convection, and this results in two coupled first-order partial differential equations describing the transfer in each of the two periods of operation. The number of variables in each system was reduced by defining dimensionless groups and normalized temperatures, and it was at this point that separate theories were developed for each of the two regenerator systems—fixed bed and rotary.

A. Regenerator Parameters

The fixed-bed system is represented by the dimensionless length Λ and the dimensionless period Π of each period. These were proposed by

Copyright © 1990 by Academic Press, Inc.
All rights of reproduction in any form reserved.